Spatial Mapping of Benzalkonium Biotransformation Pathways in Wastewater Biofilms

Prasad B Phapale[a], Dionysios D. Neofytos[b], Yrsa Larsson, Milena Corredig[b], Kai Bester*

Supplementary Figures

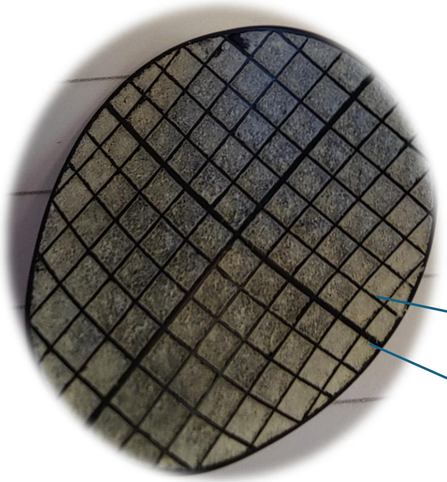

z-MBBR Biofilm carriers

a)

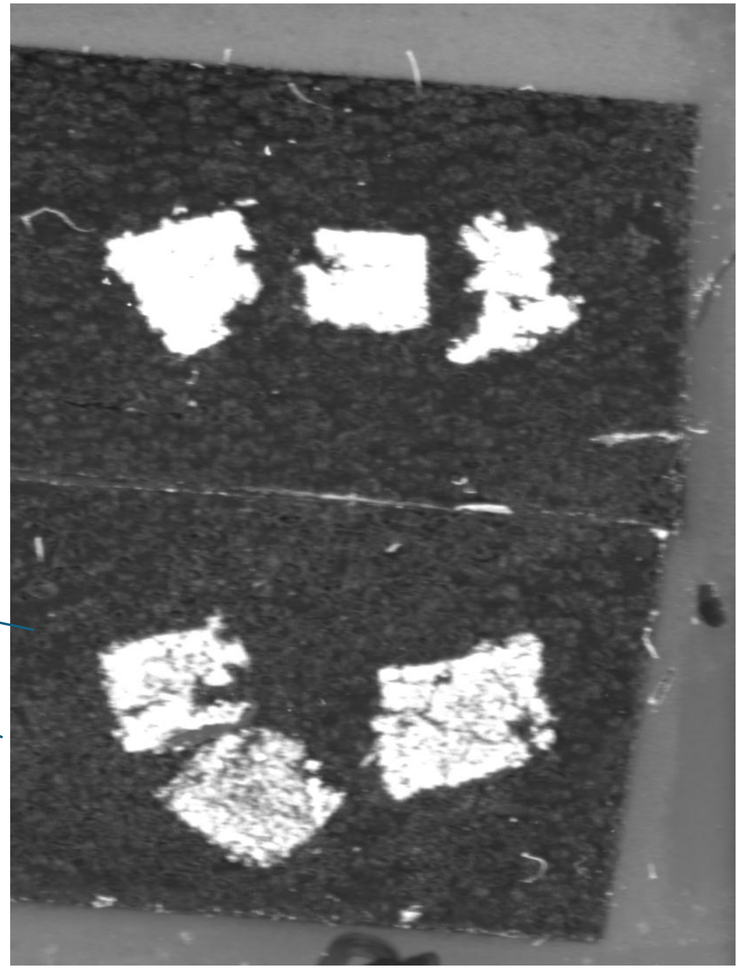

b)

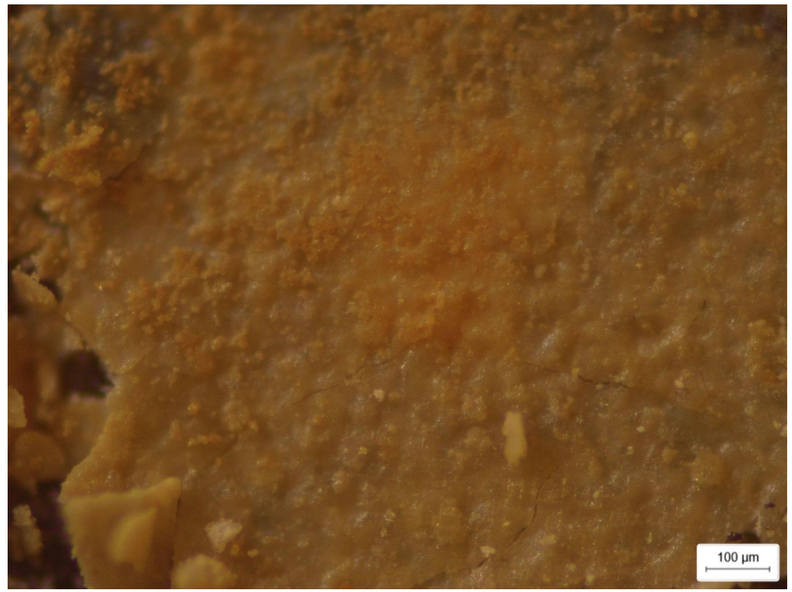

c)

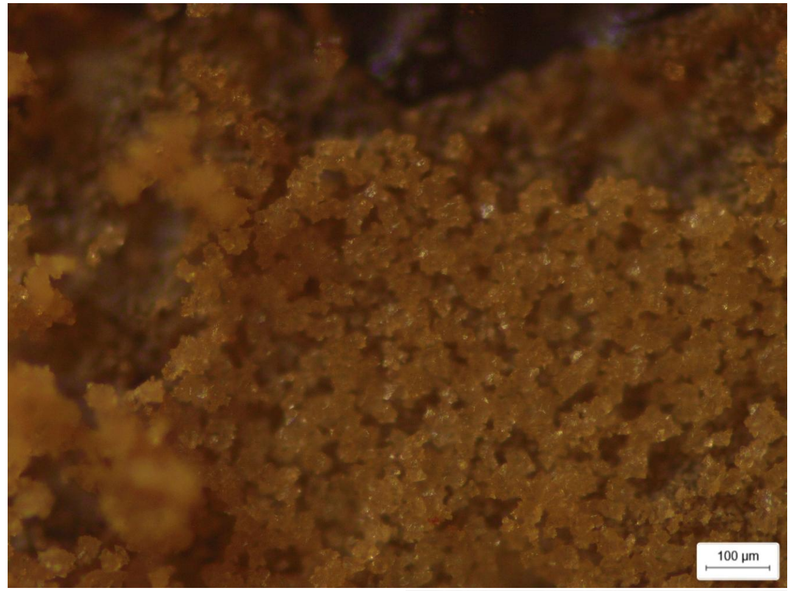

d)

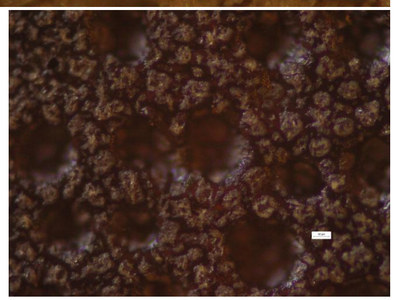

Supplementary Fig. 1 a) Biofilms mounted on ITO slides using conductive carbon tape. b) Microscopic images of a biofilm region (10x magnification) removed from MBBR carriers and desiccated, c) a biofilm image after application of MALDI matrix, d) MALDI laser ablation marks post MS imaging data acquisition.

BAC12

C21H38N

304.3004

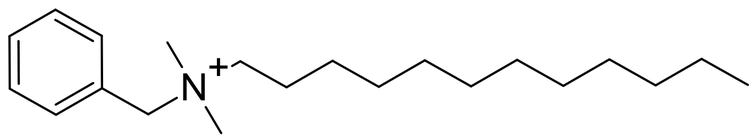

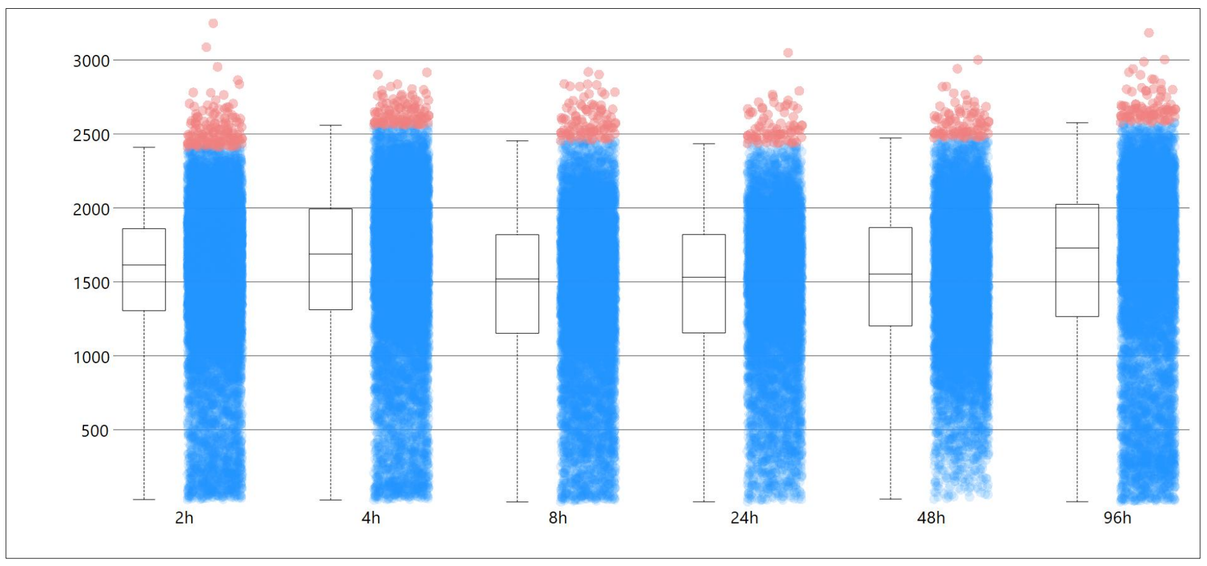

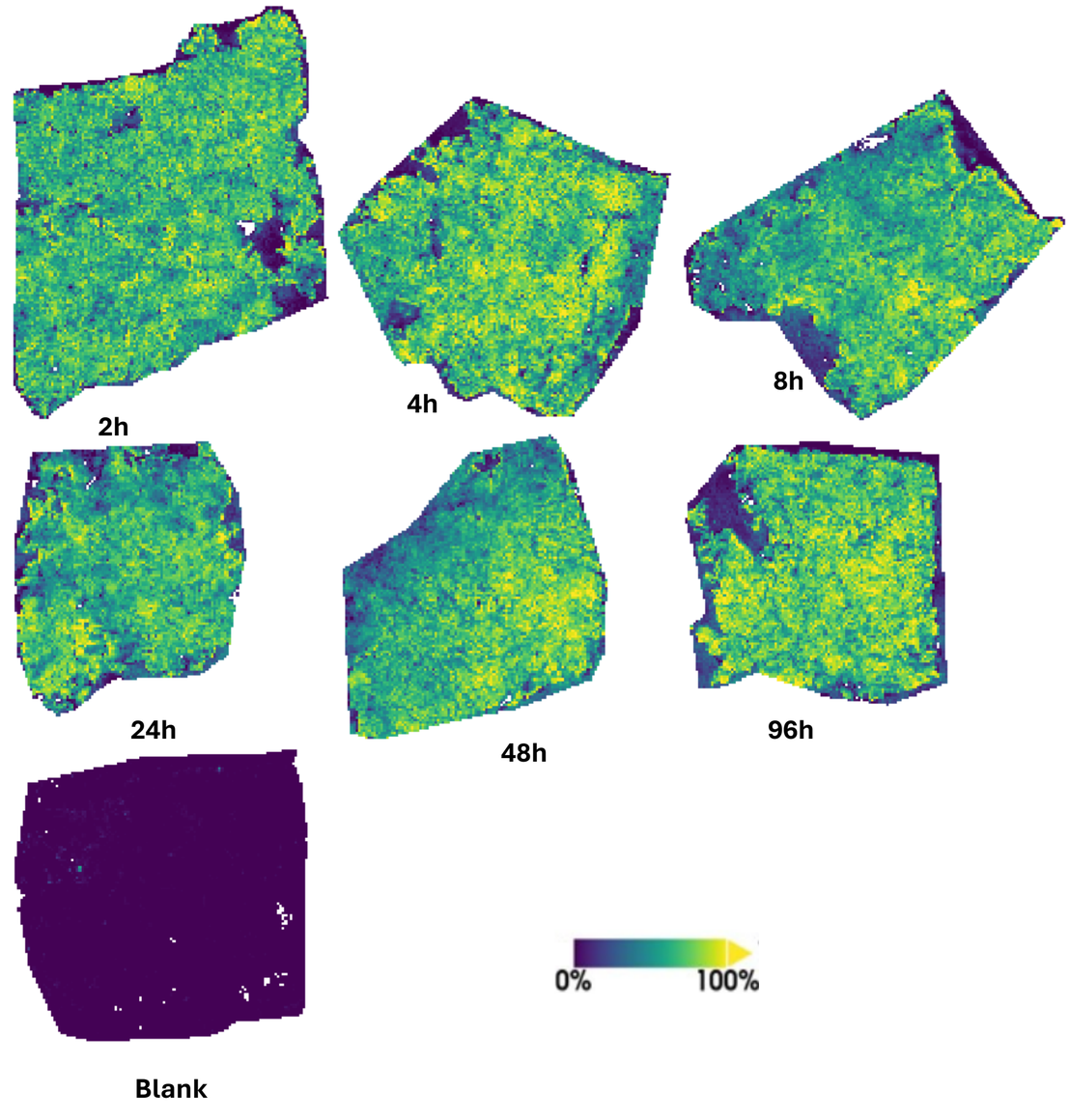

Supplementary Fig. 2) MS Ion images of BAC-12 (RMS normalized) over the time-course of 2, 4, 8, 24, 48, 96 h.

BAC12-aldehyde

318.2797

C21H36NO

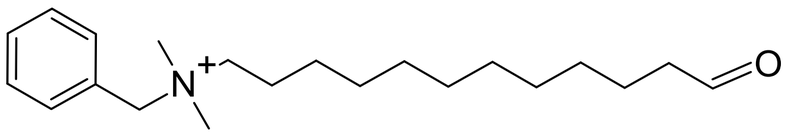

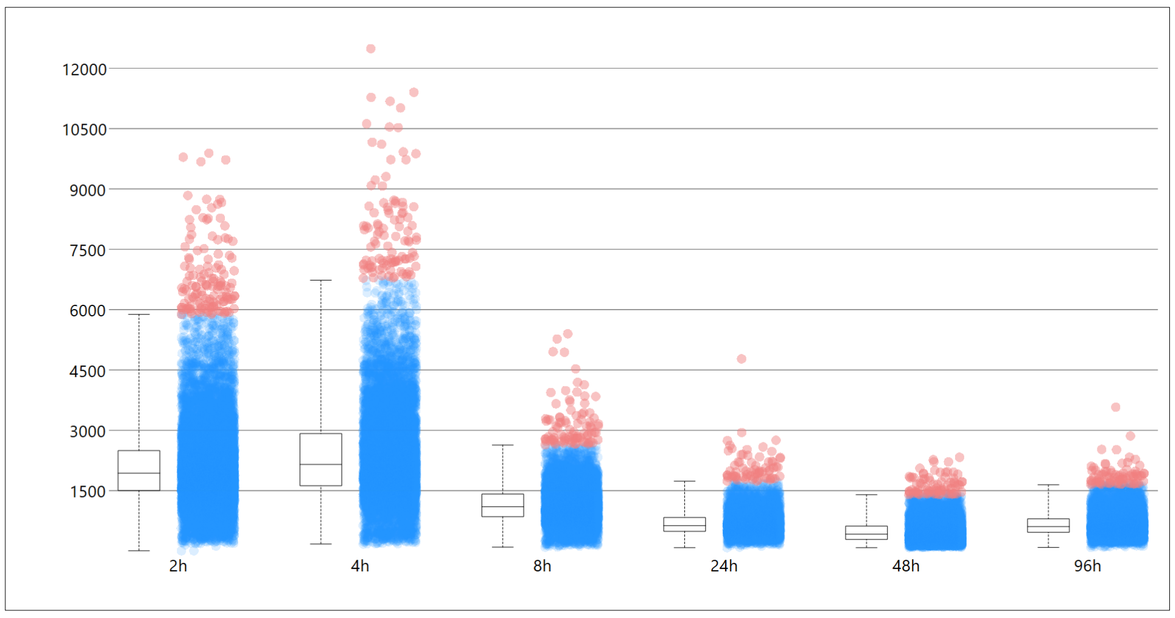

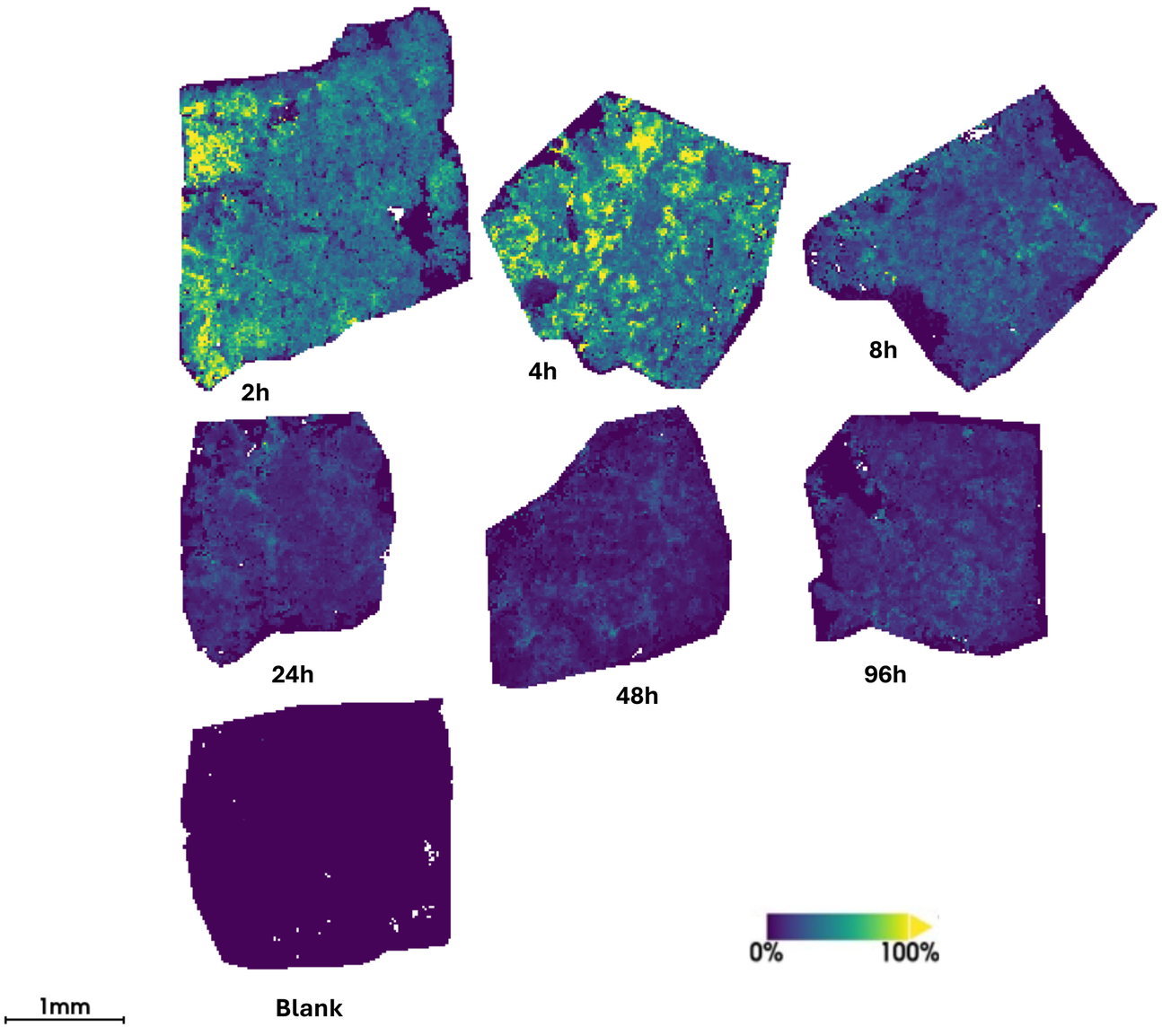

Supplementary Fig. 3a) MS Ion images of BAC12-ω-aldehyde over the time-course of 2, 4, 8, 24, 48, 96 h.

BAC12-OH

320.2921

C21H38NO

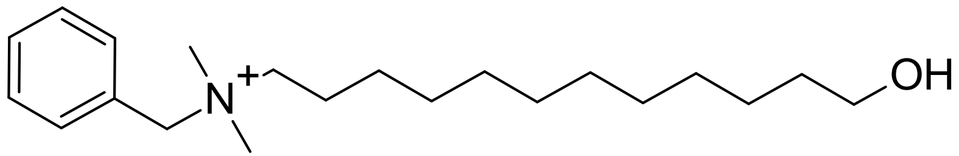

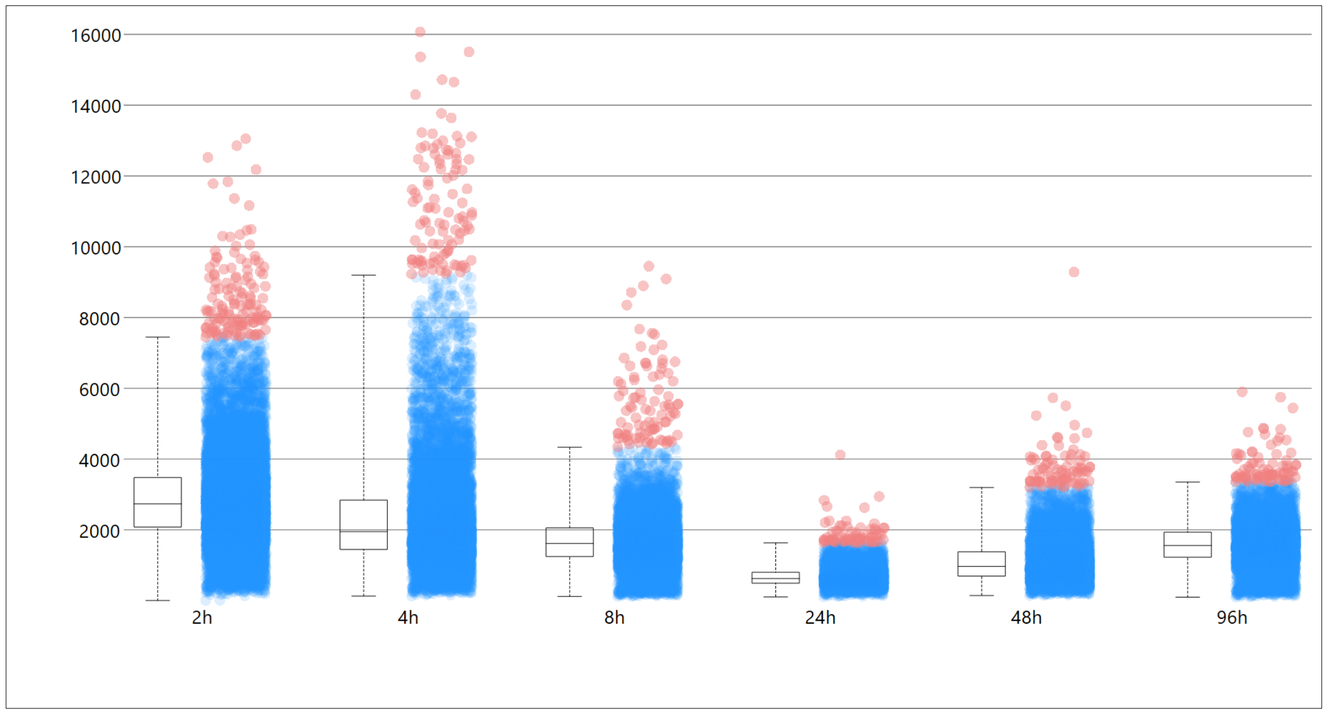

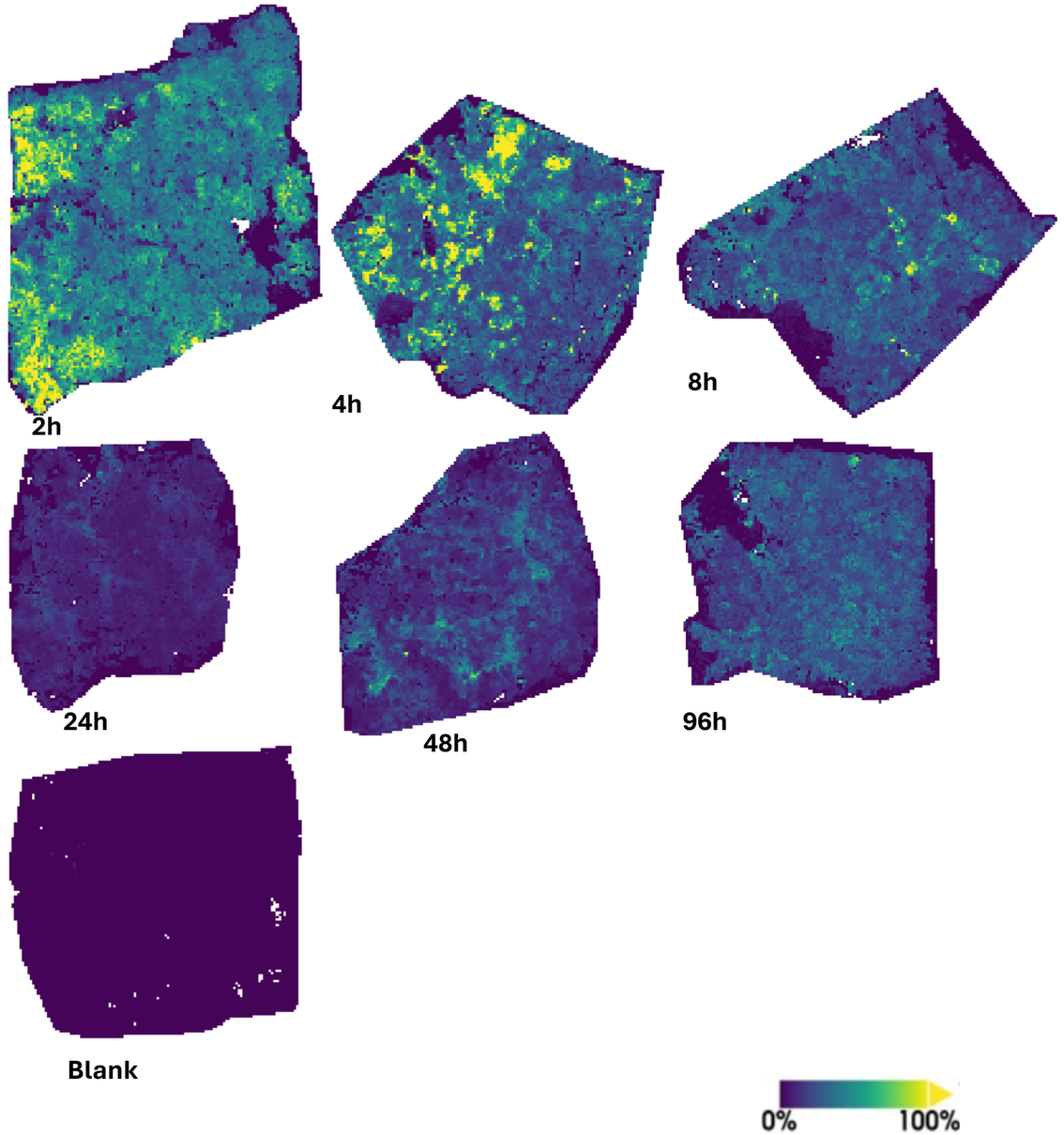

Supplementary Fig. 3b) MS Ion images of BAC12-OH over the time-course of 2, 4, 8, 24, 48, 96 h.

BAC12-carboxy

334.2746

C21H36NO2

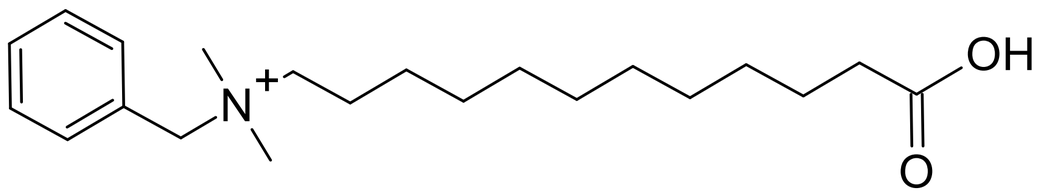

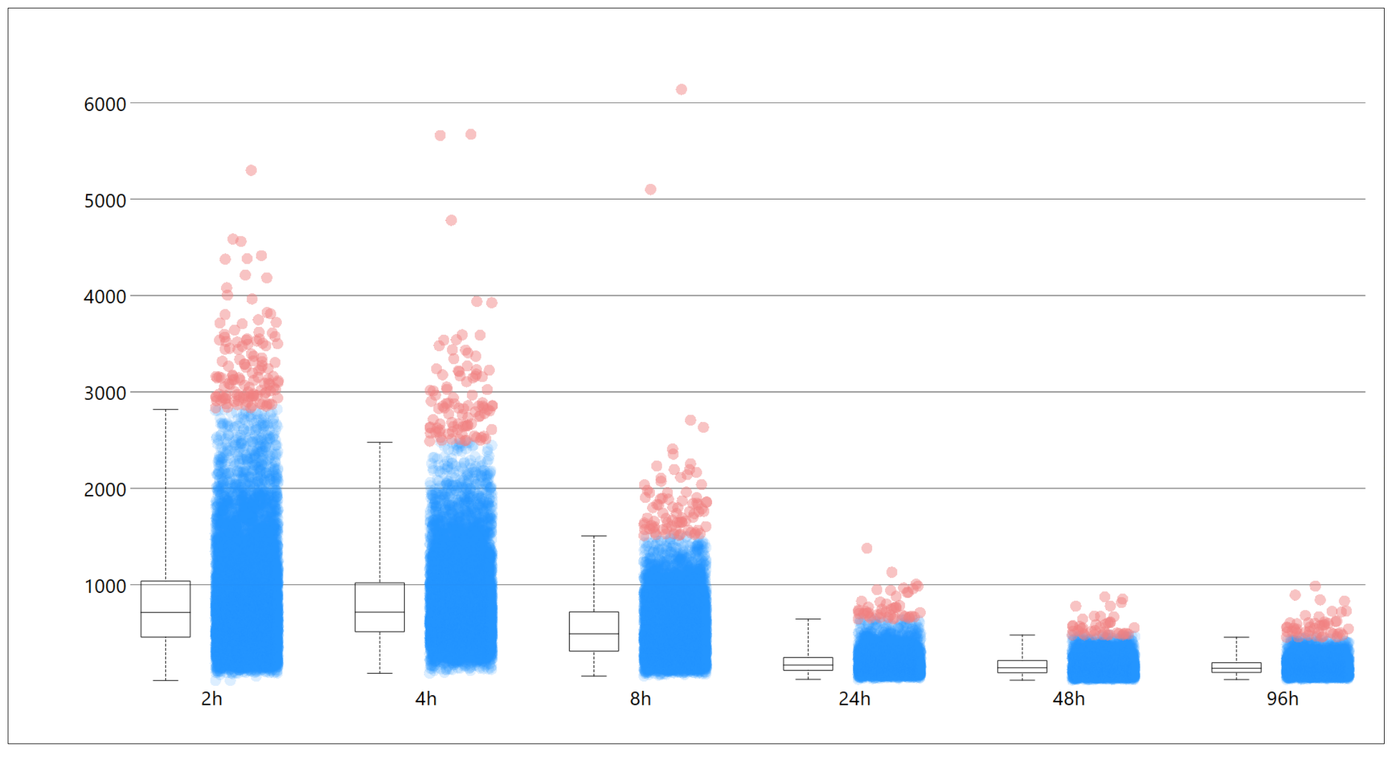

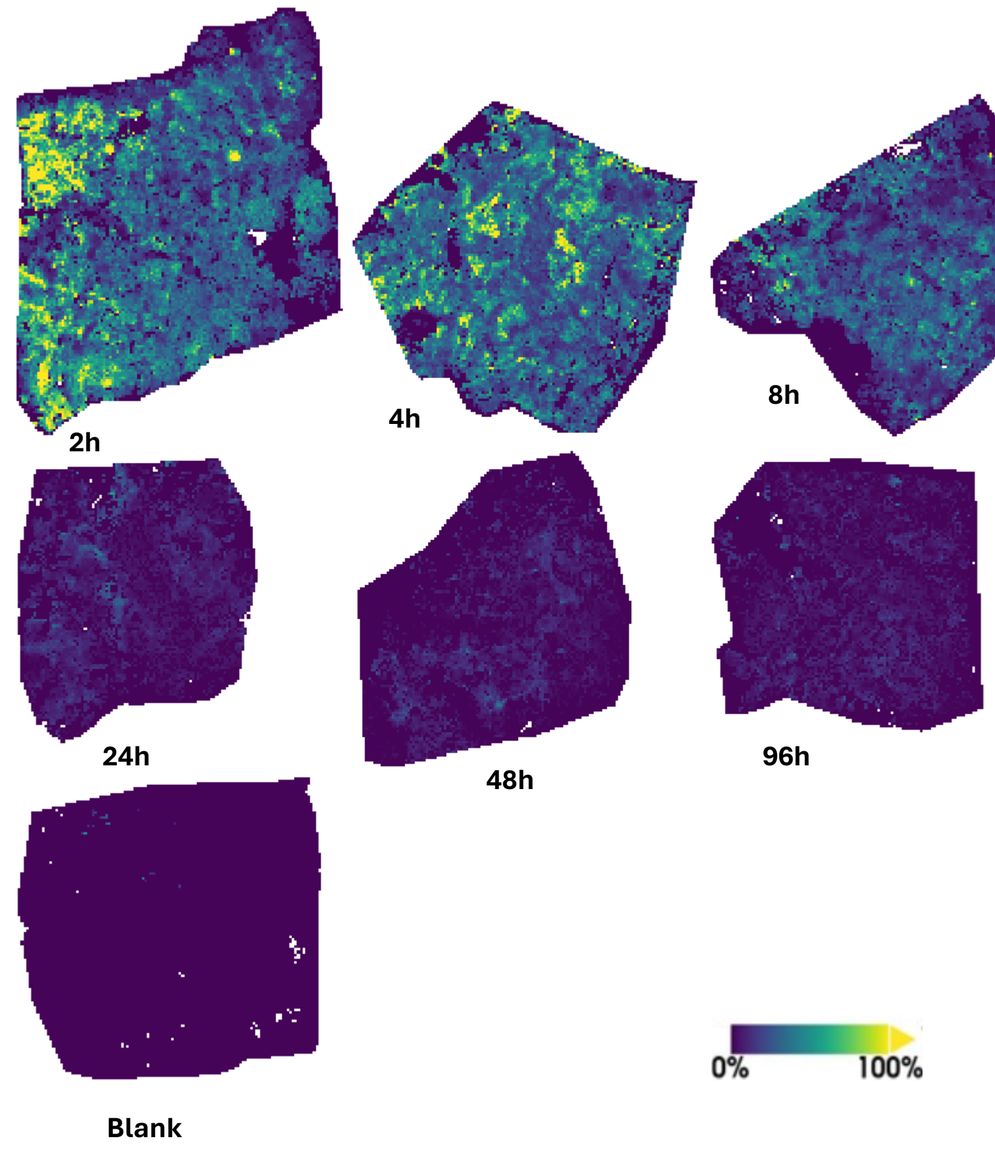

Supplementary Fig. 3c) MS Ion images of BAC12-ω-carboxy over the time-course of 2, 4, 8, 24, 48, 96 h.

BAC12-diOH

336.2905

C21H38NO2

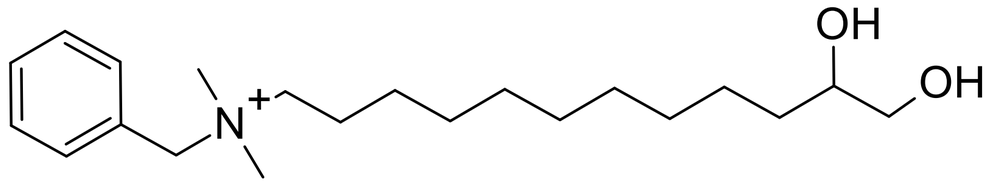

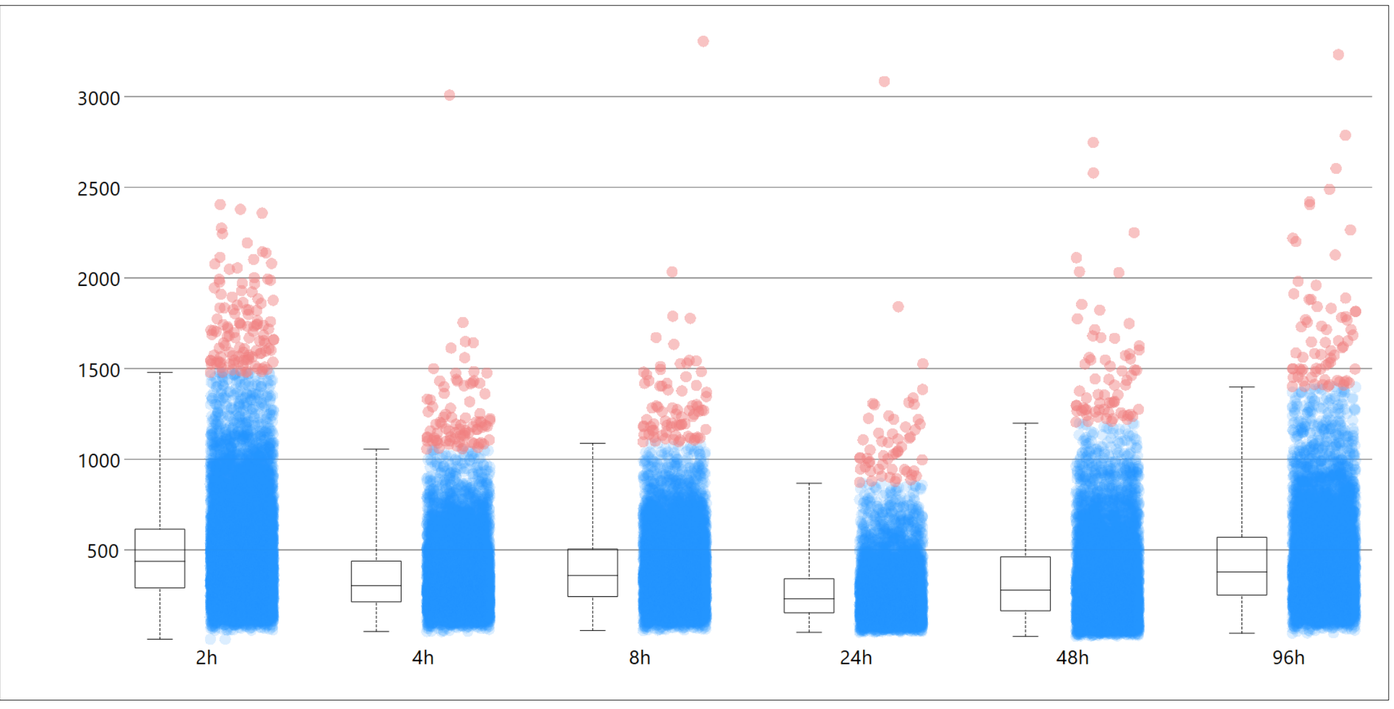

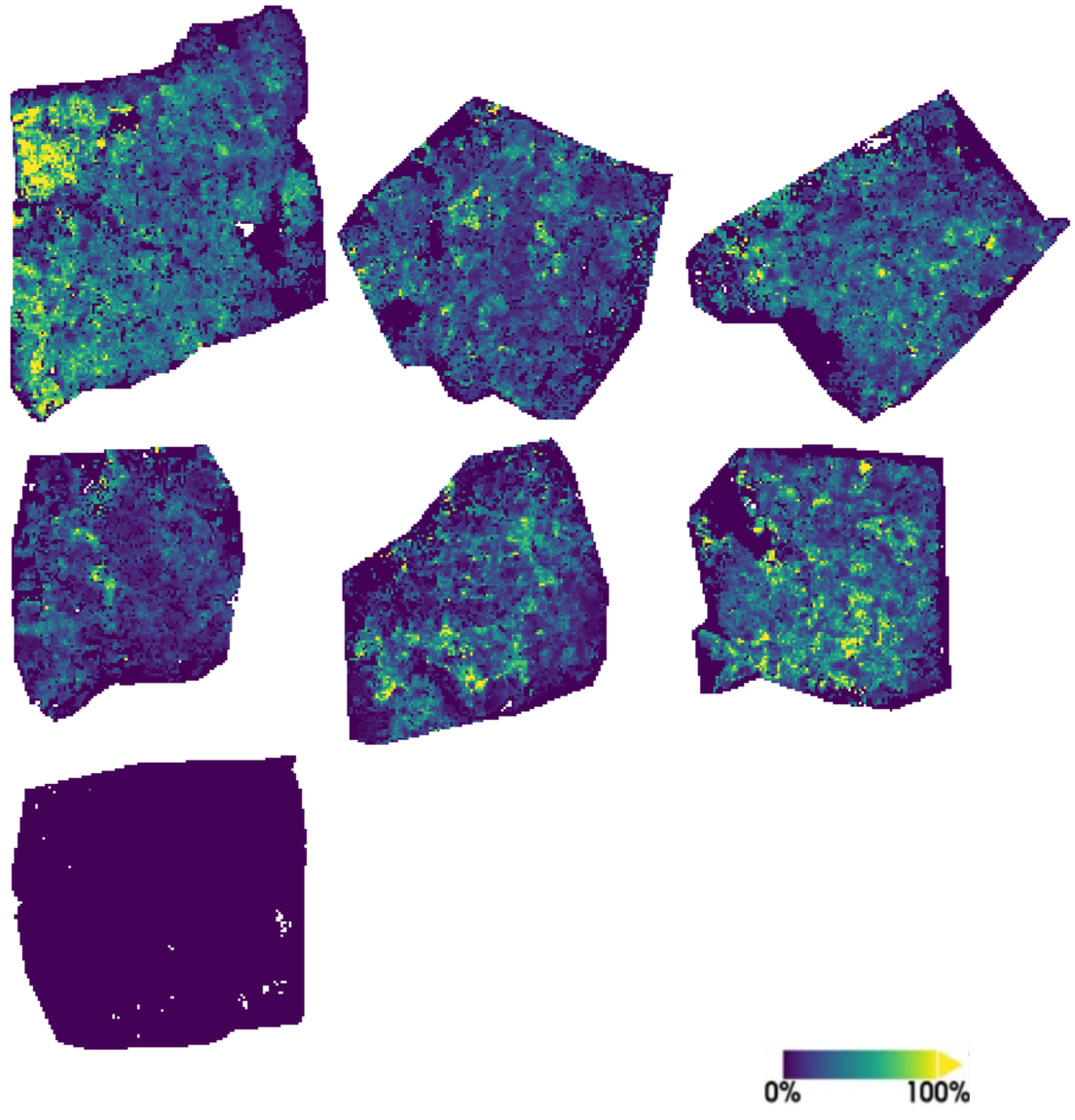

Supplementary Fig. 3d) MS Ion images of BAC12-diOH over the time-course of 2, 4, 8, 24, 48, 96 h.

BAC12-unsat-carboxy

332.2589

C21H34NO2

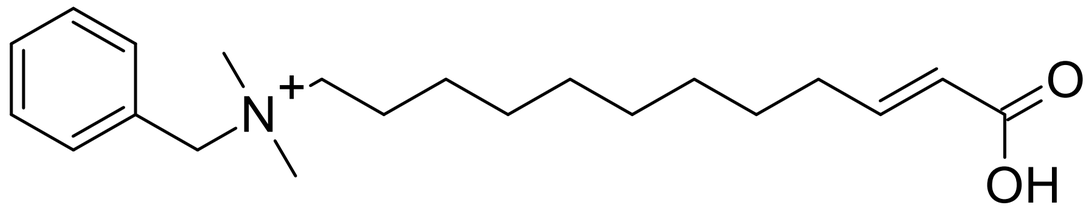

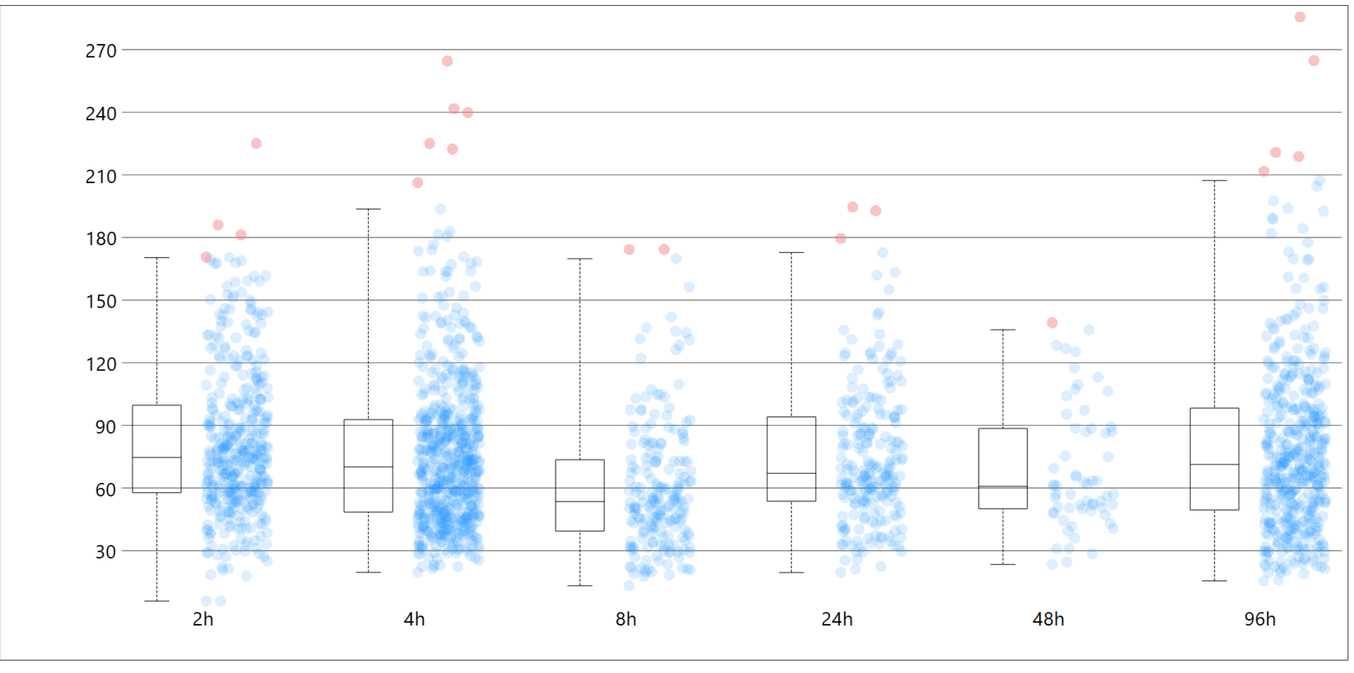

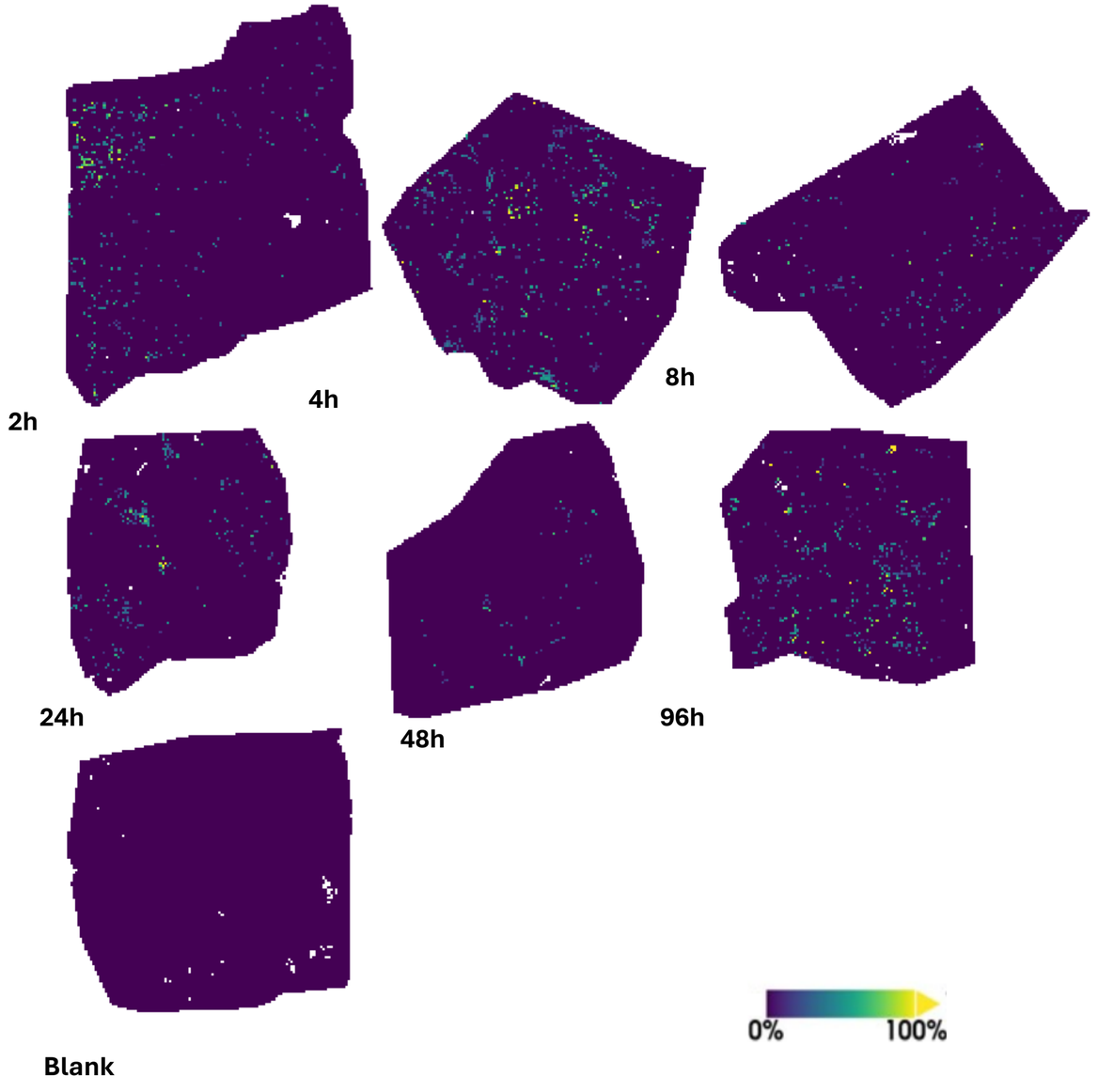

Supplementary Fig. 3e) MS Ion images of BAC12-unsat-carboxy over the time-course of 2, 4, 8, 24, 48, 96 h.

BAC10-unsat-carboxy

304.2271

C19H30NO2

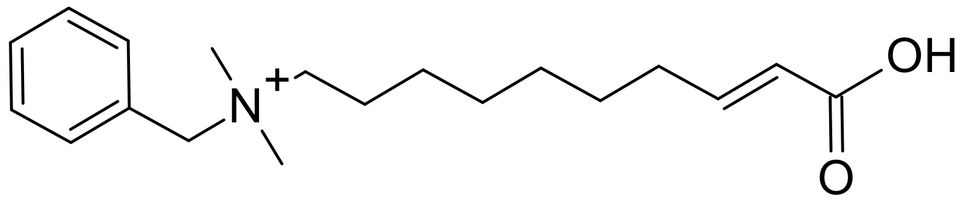

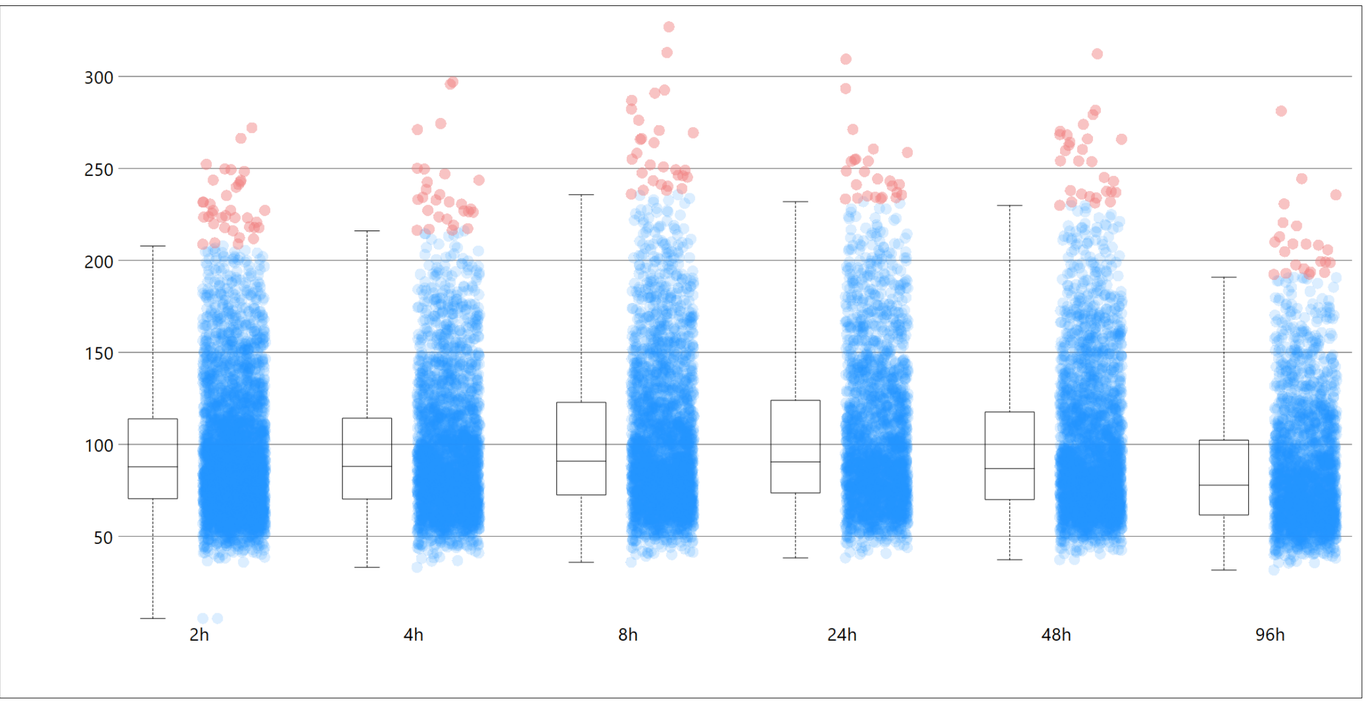

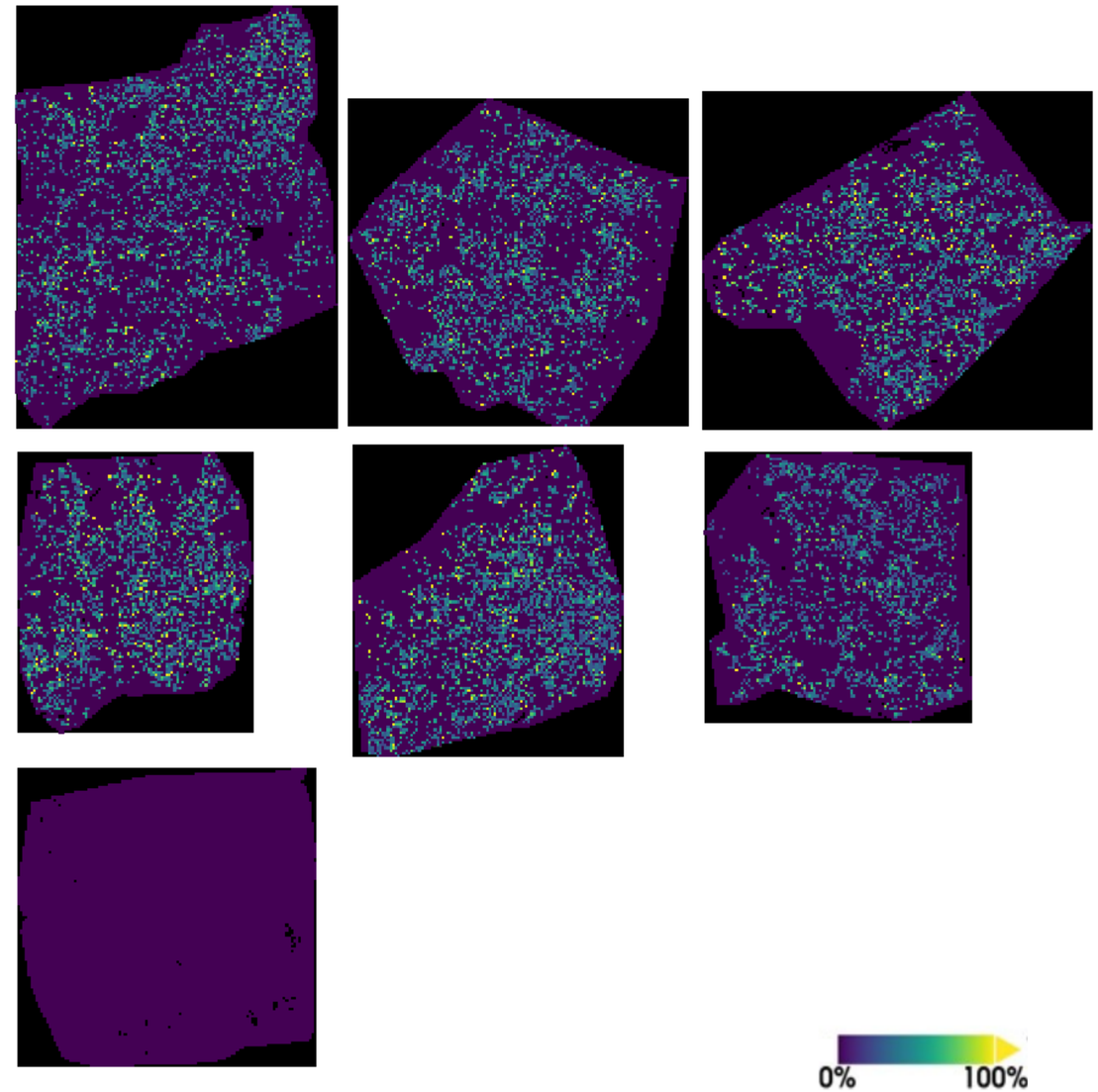

Supplementary Fig. 3f) MS Ion images of BAC10-unsat-carboxy over the time-course of 2, 4, 8, 24, 48, 96 h.

BAC10-carboxy

306.2433

C19H32NO2

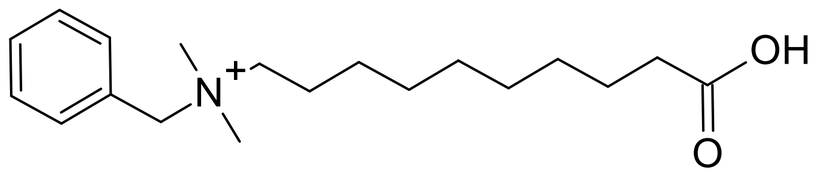

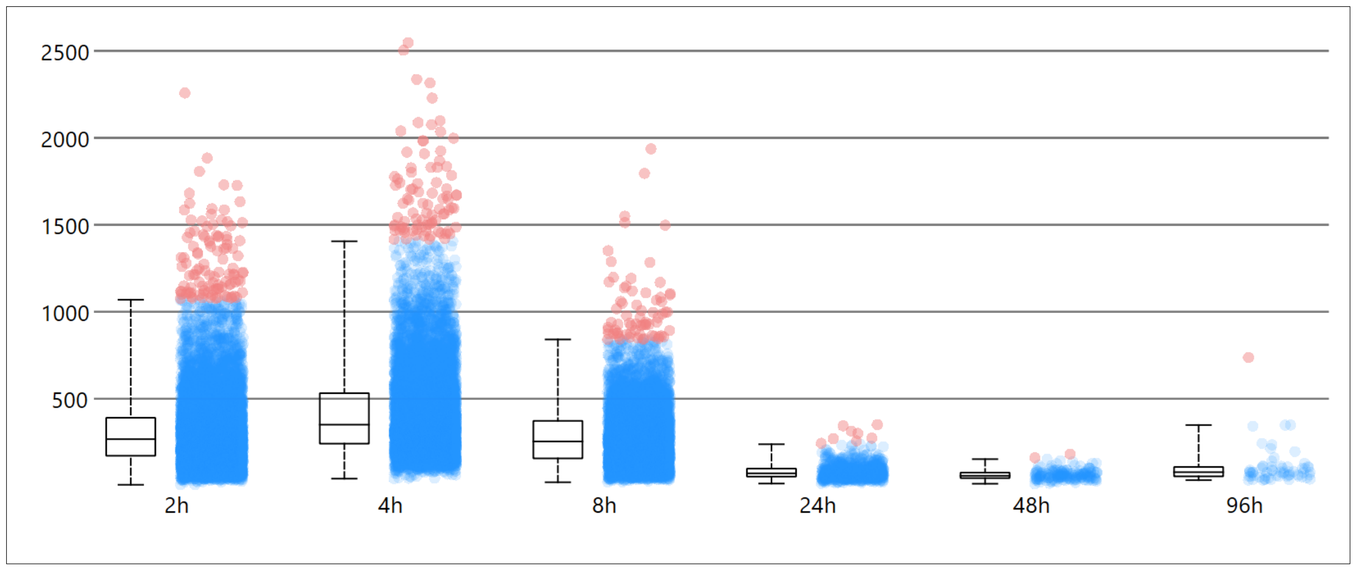

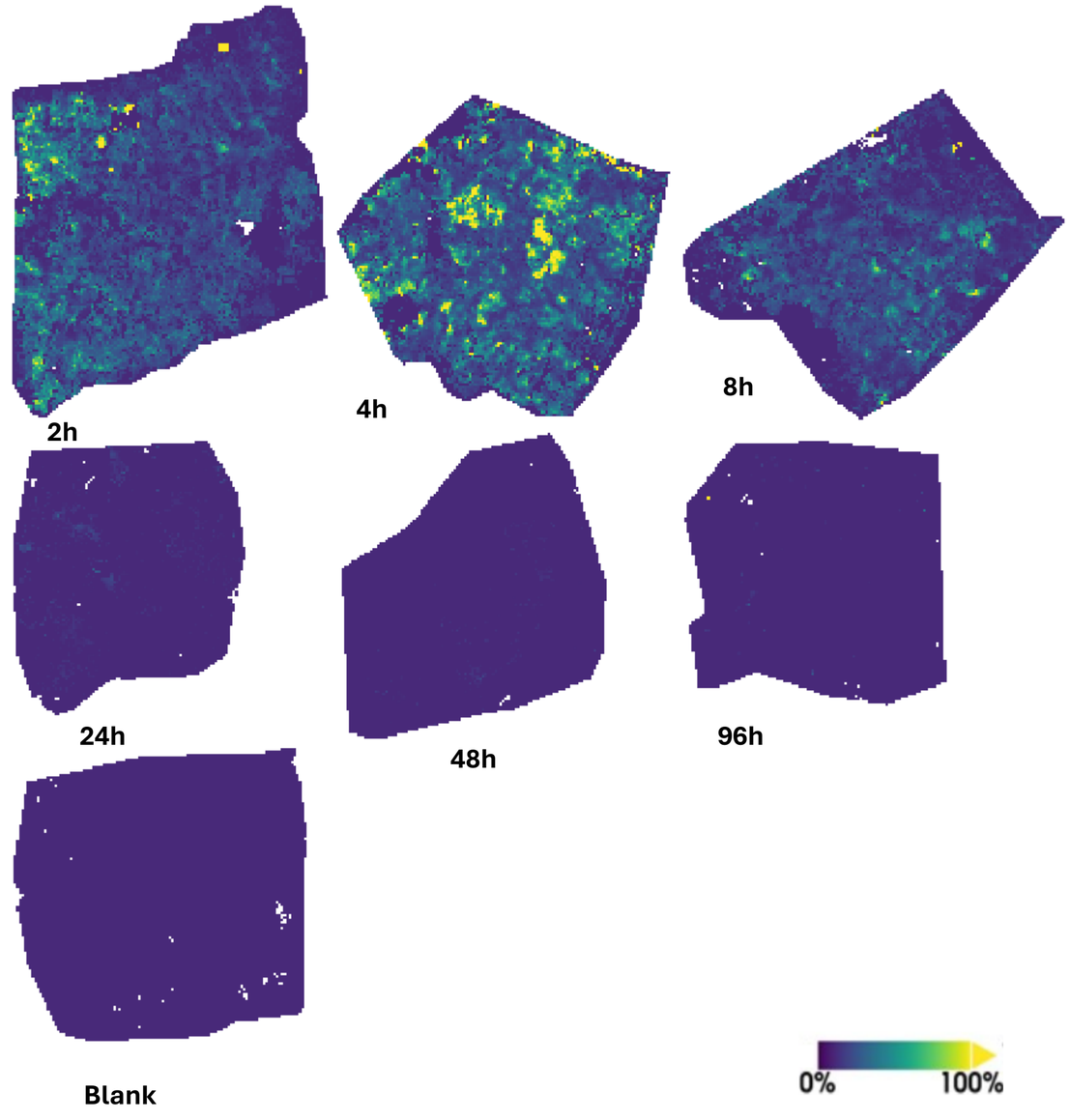

Supplementary Fig. 3g) MS Ion images of BAC10-carboxy over the time-course of 2, 4, 8, 24, 48, 96 h.

BAC9-carboxy

292.2278

C18H30NO2

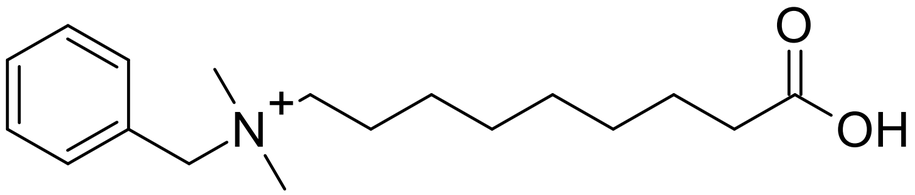

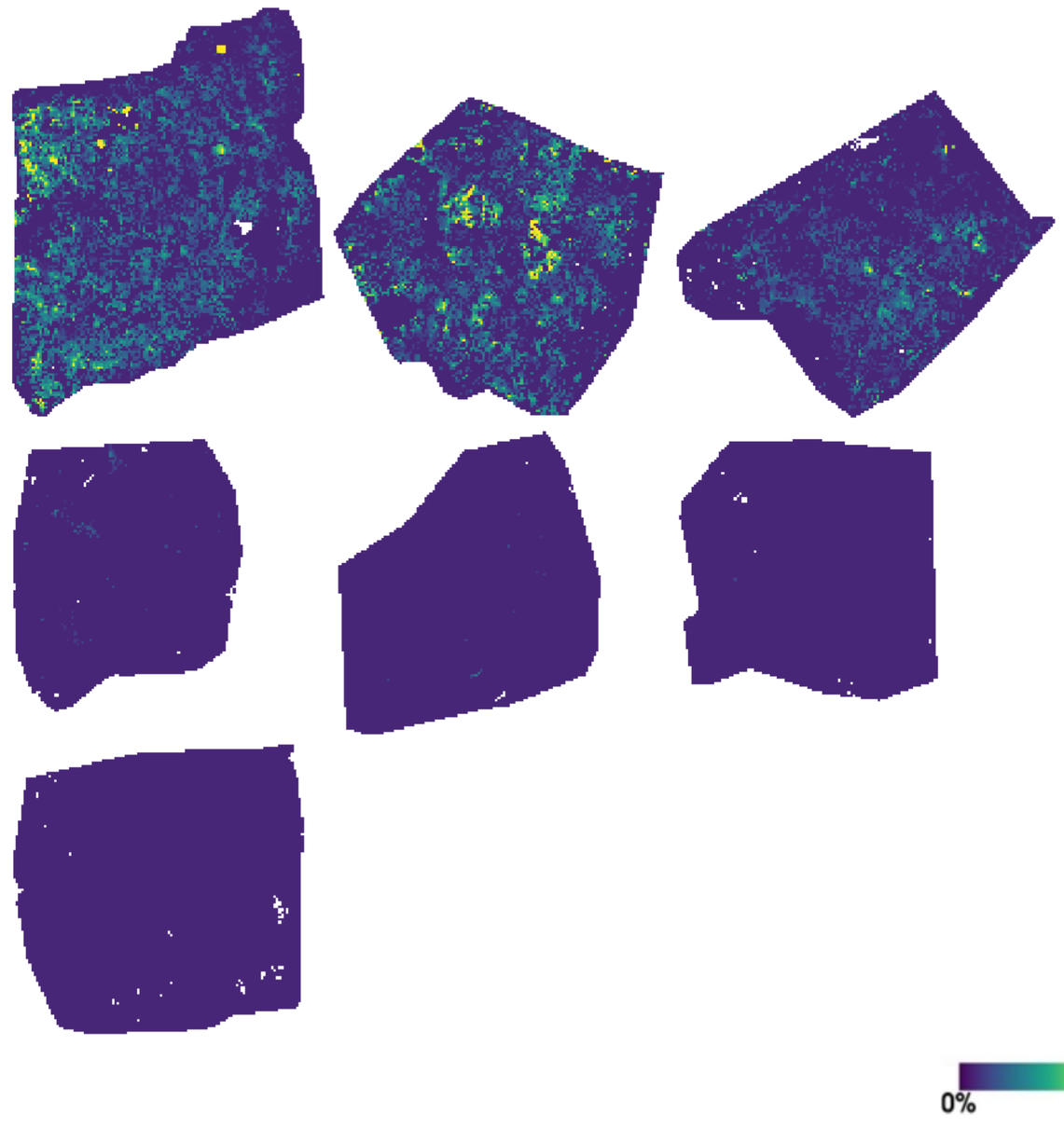

Supplementary Fig. 3h) MS Ion images of BAC9-carboxy over the time-course of 2, 4, 8, 24, 48, 96 h

BAC6-carboxy

250.1714

C15H24NO2

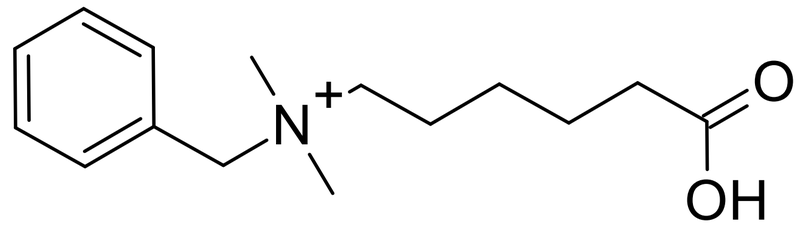

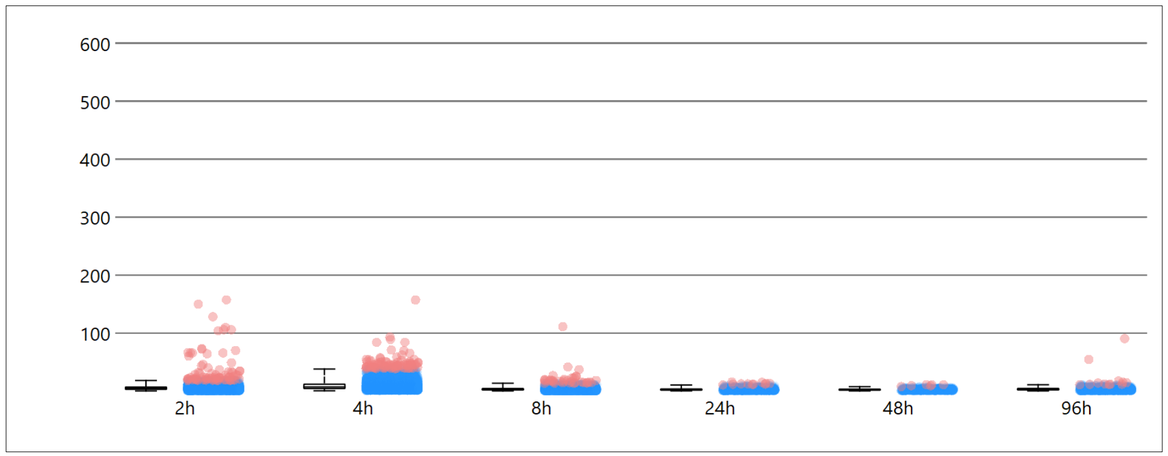

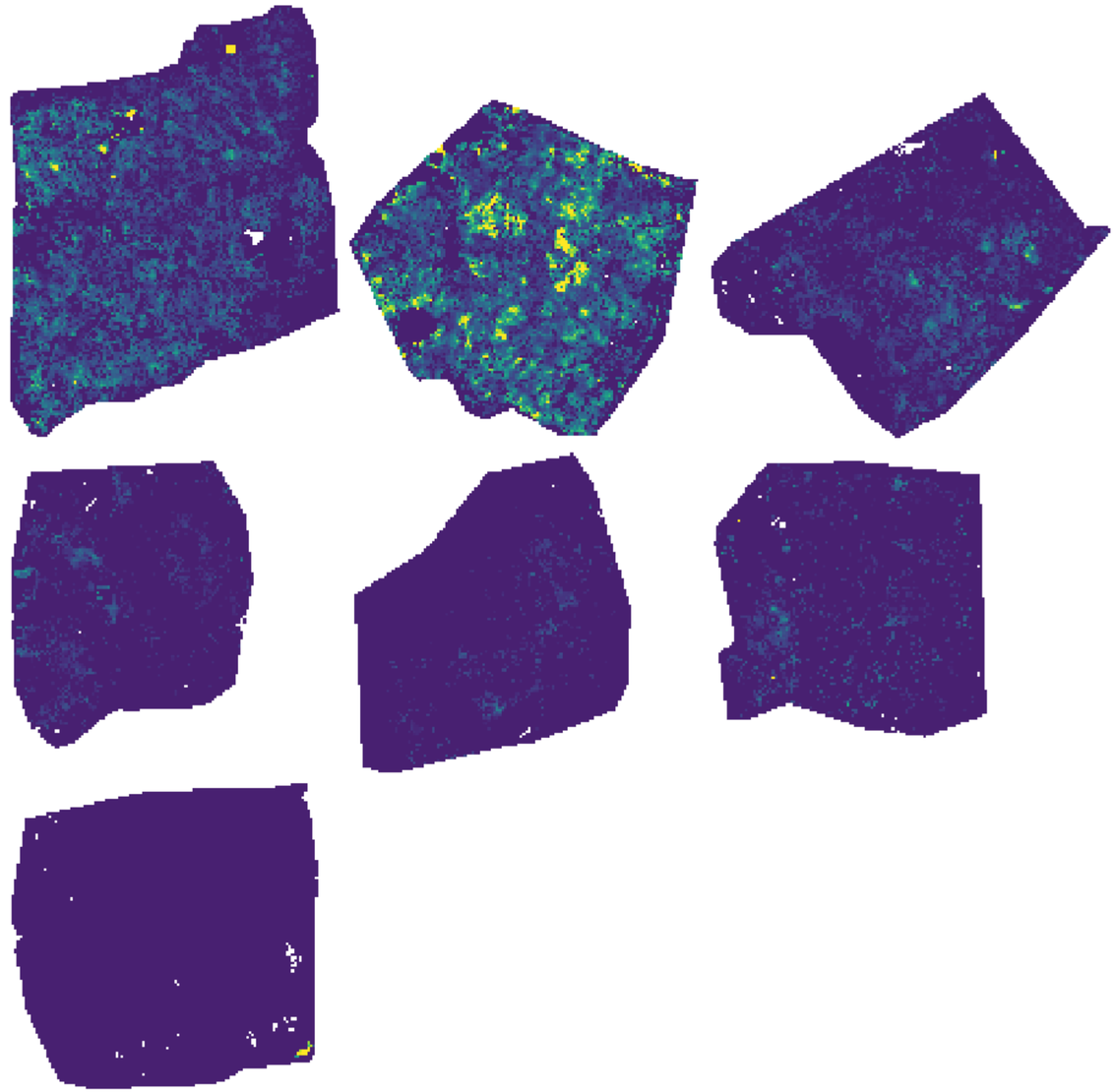

Supplementary Fig. 3i) MS Ion images of BAC6-carboxy over the time-course of 2, 4, 8, 24, 48, 96 h.

BAC7-carboxy

264.1963

C16H26NO2

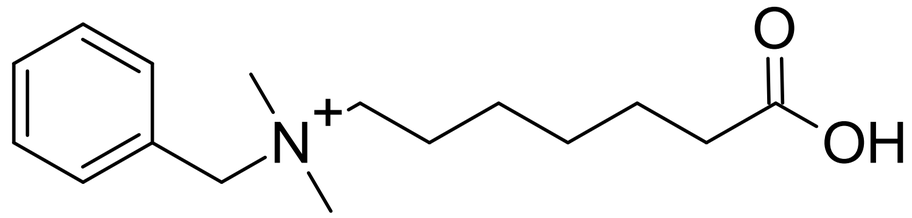

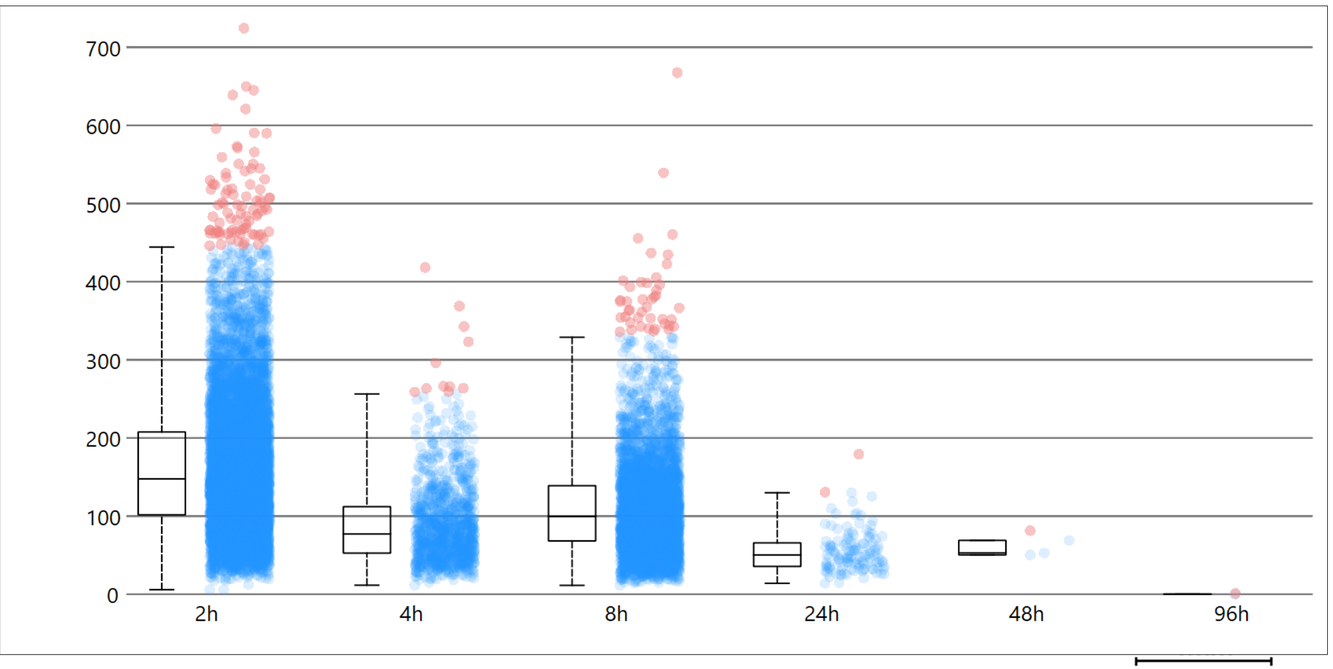

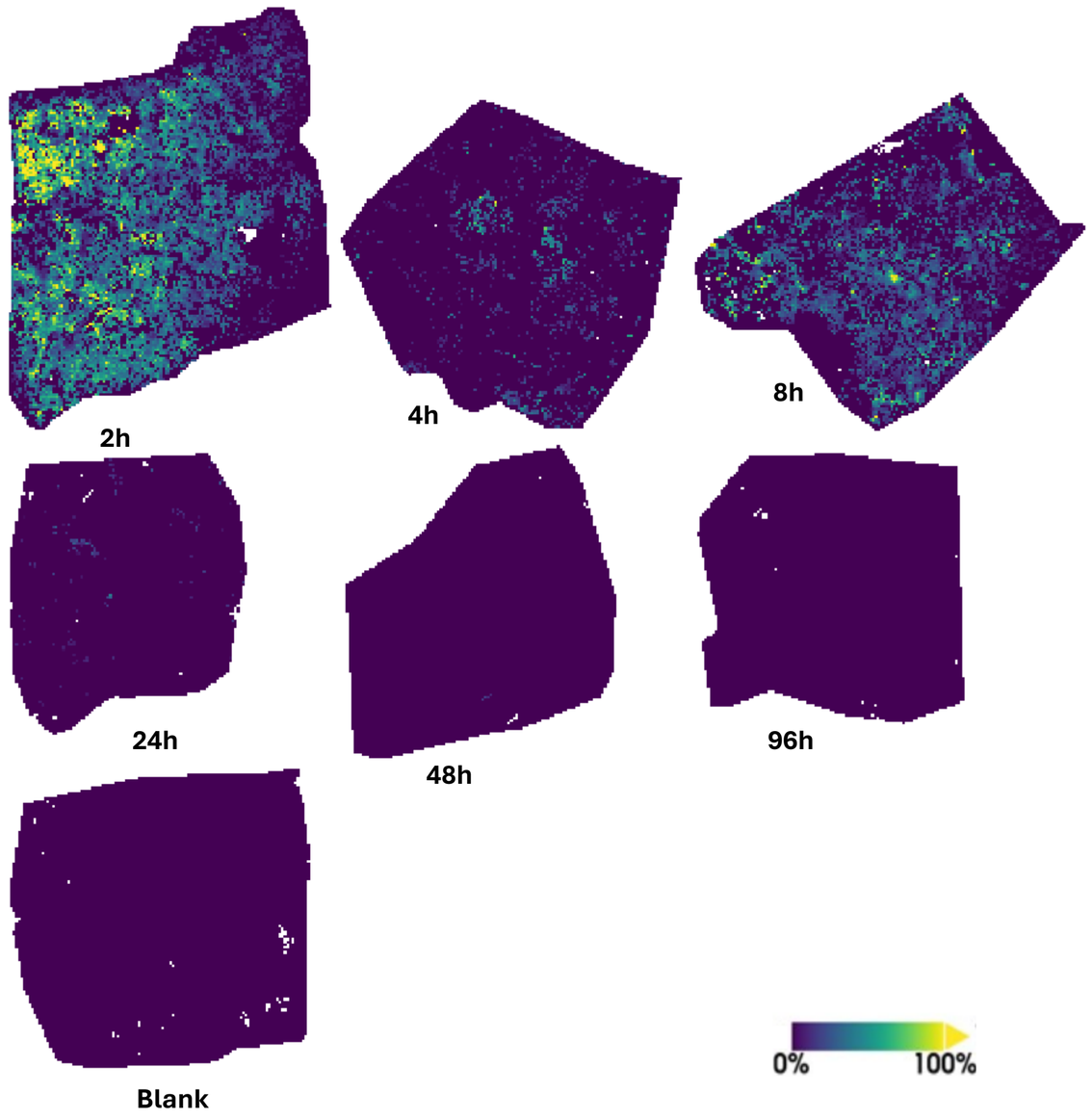

Supplementary Fig. 3j) MS Ion images of BAC7-carboxy over the time-course of 2, 4, 8, 24, 48, 96 h.

BAC8-carboxy

278.2122

C17H28NO2

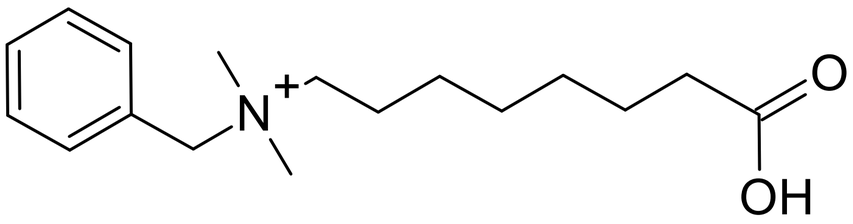

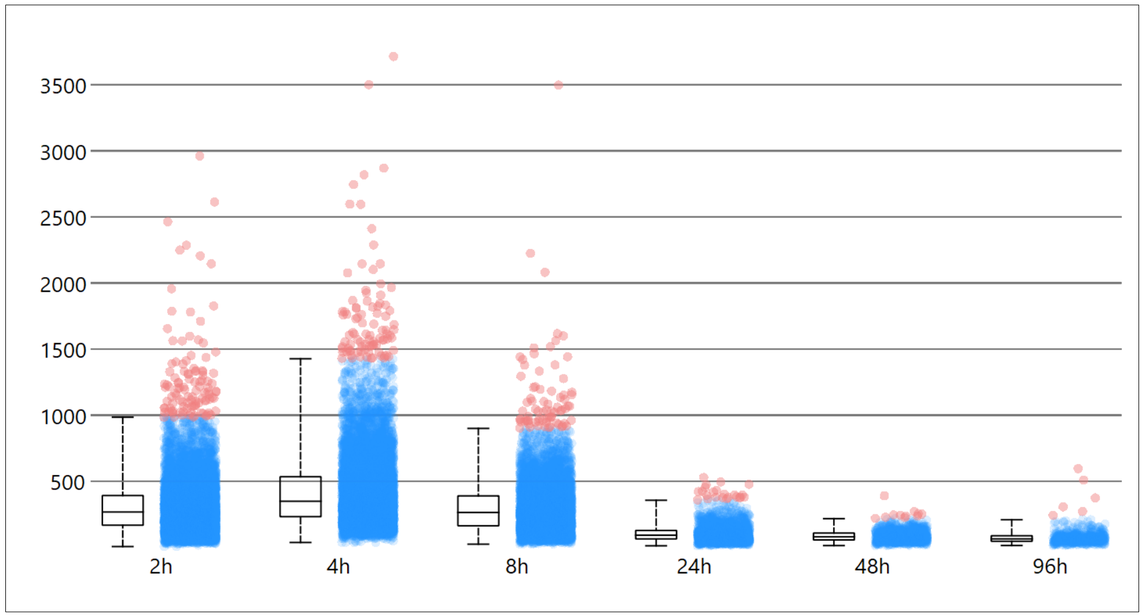

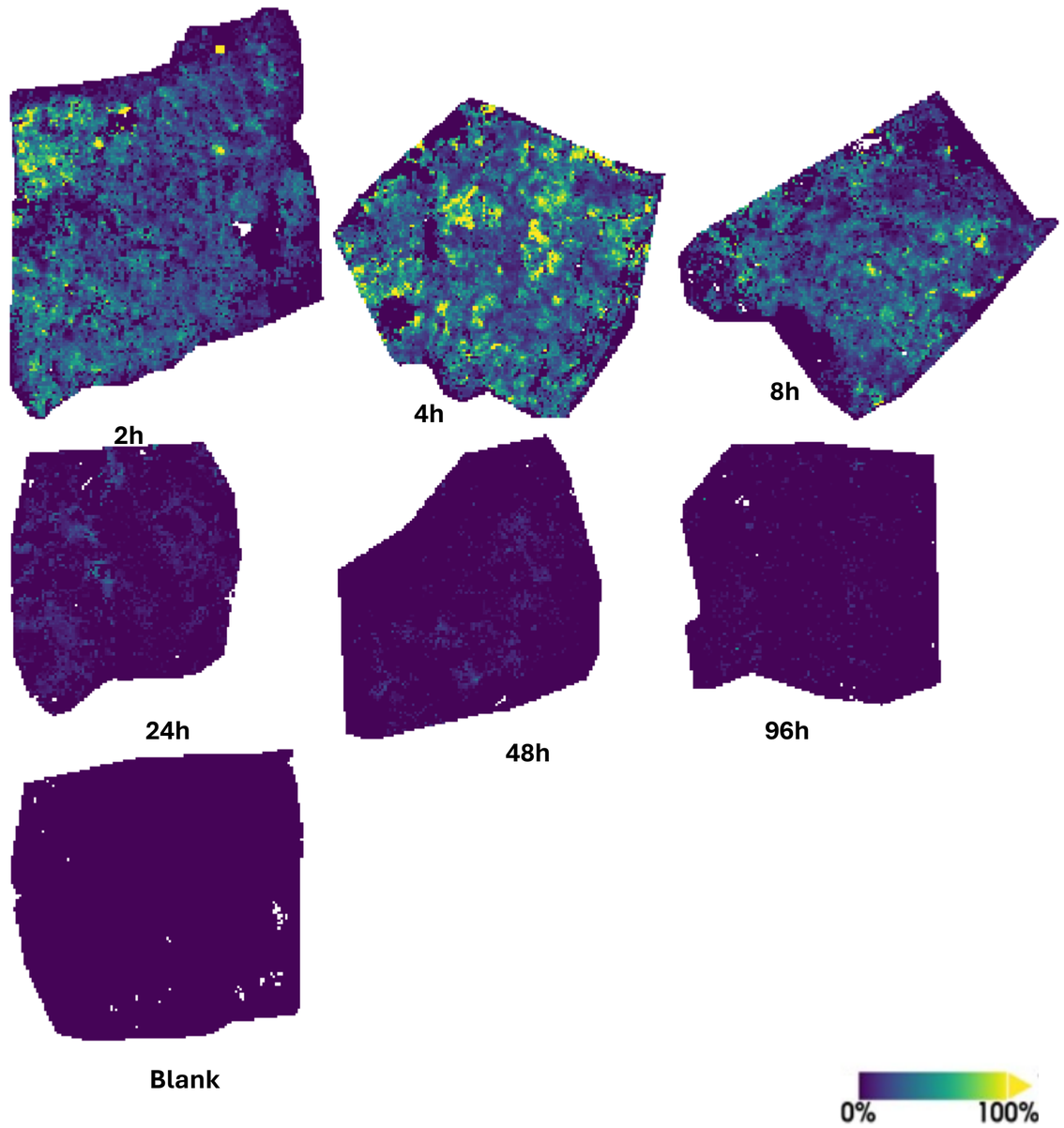

Supplementary Fig. 3k) MS Ion images of BAC8-carboxy over the time-course of 2, 4, 8, 24, 48, 96 h.

BAC5-carboxy

236.1650

C14H22NO2

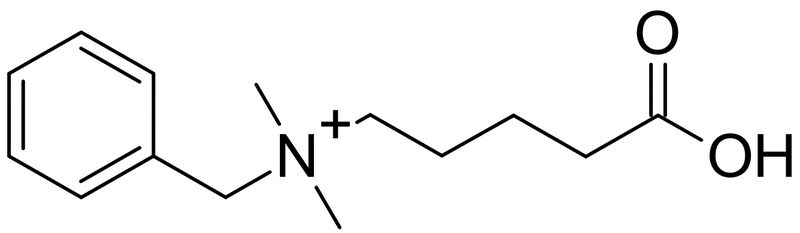

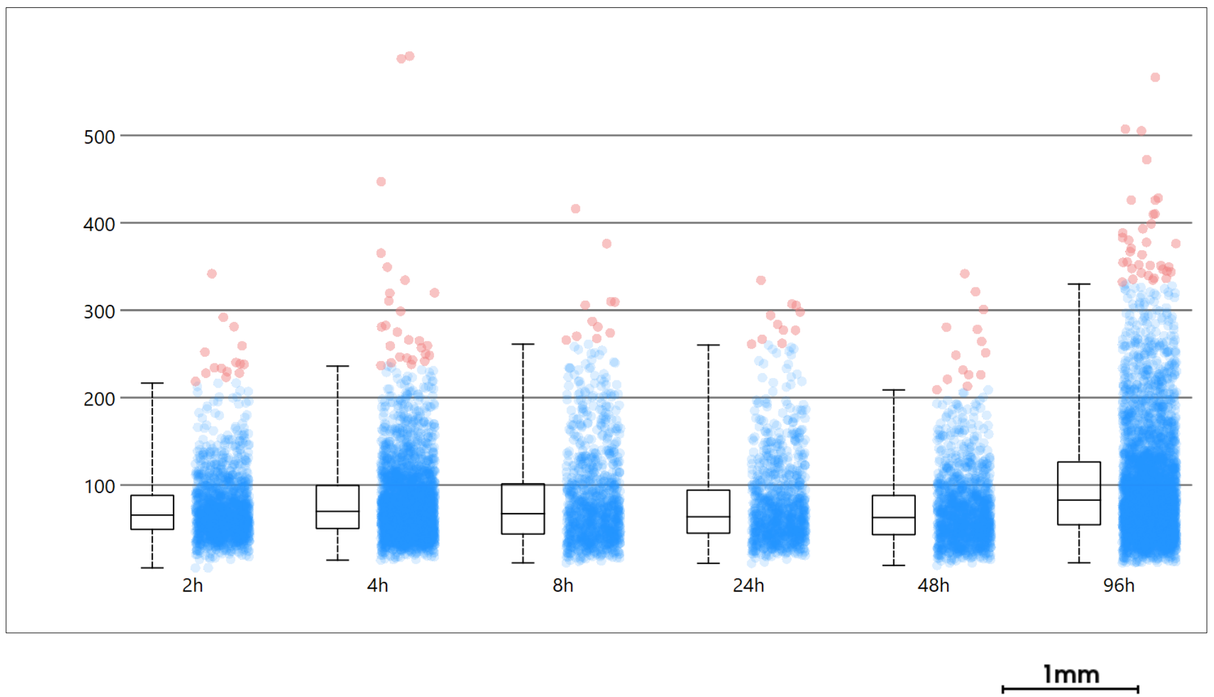

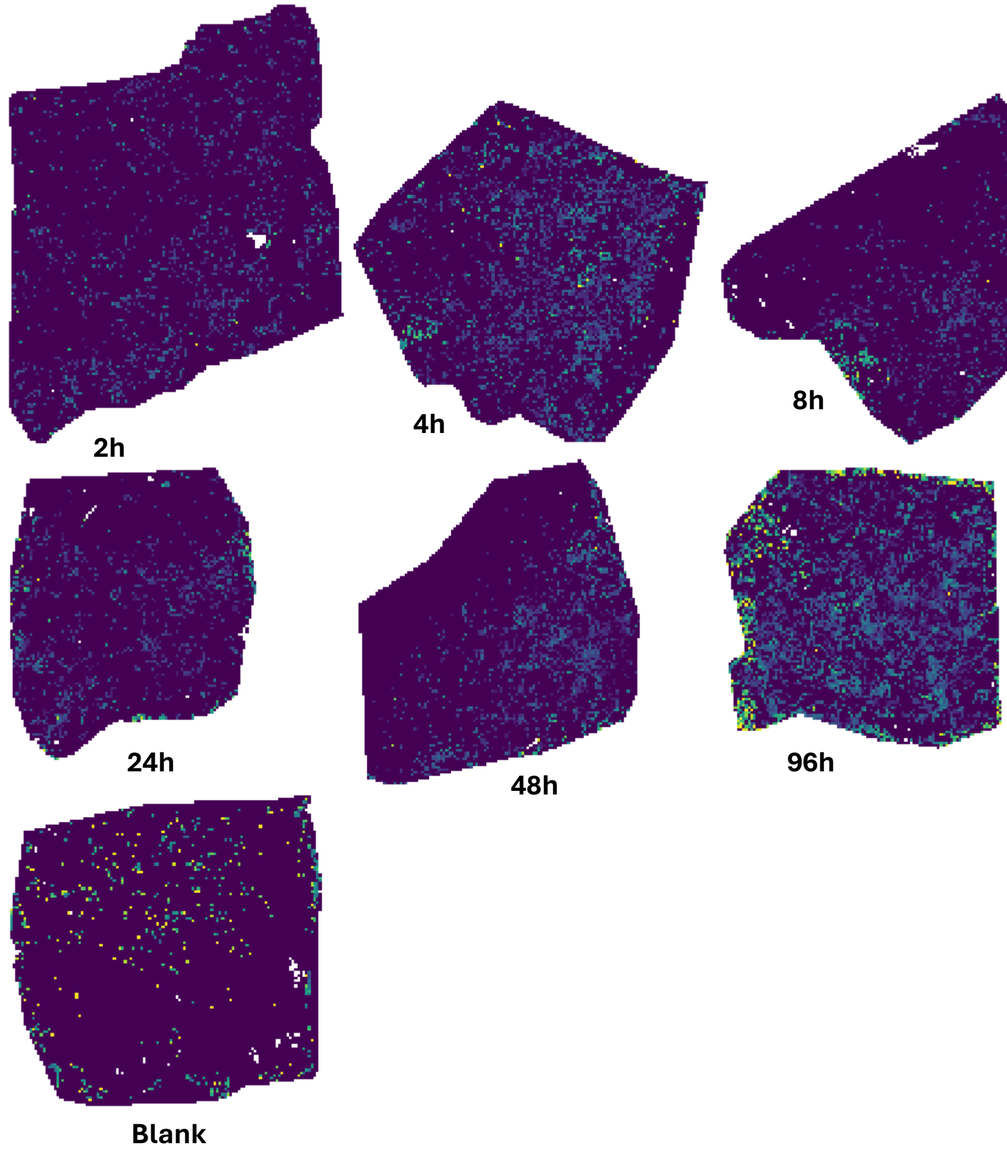

Supplementary Fig. 3l) MS Ion images of BAC5-carboxy over the time-course of 2, 4, 8, 24, 48, 96 h.

BAC5-OH

222.19213

C14H24NO

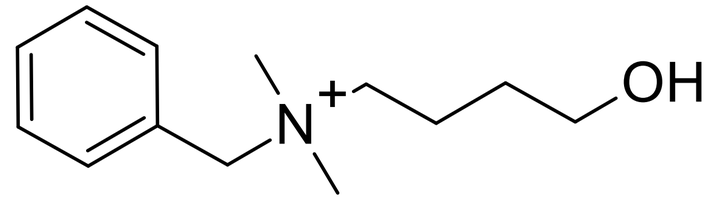

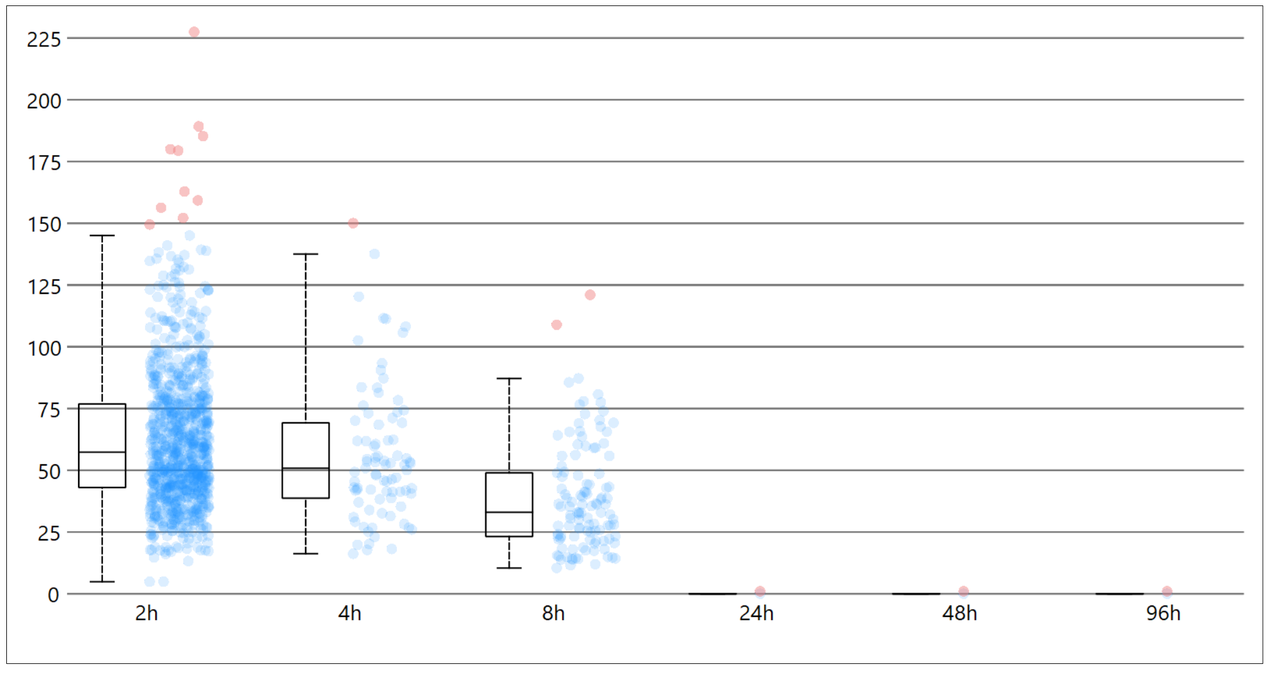

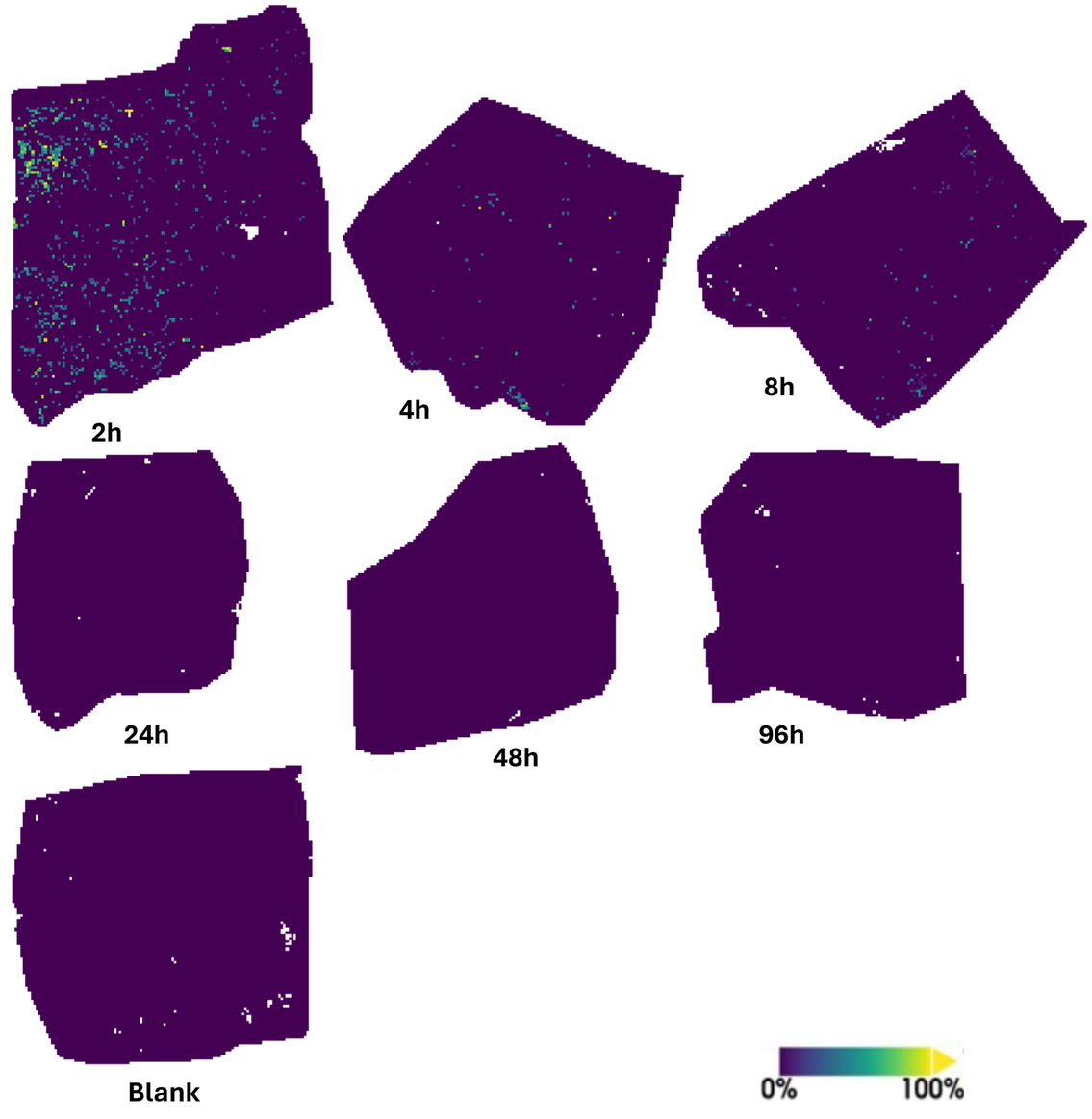

Supplementary Fig. 3m) MS Ion images of BAC5-OH over the time-course of 2, 4, 8, 24, 48, 96 h.

BAC4-OH

208.1501

C13H22NO

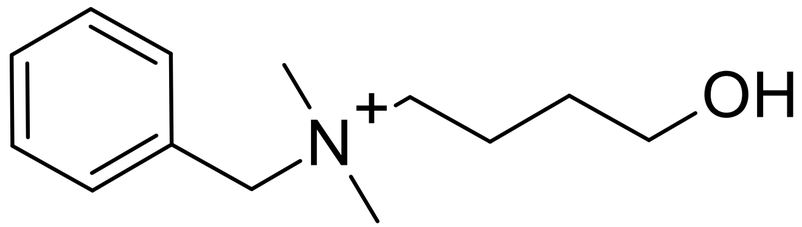

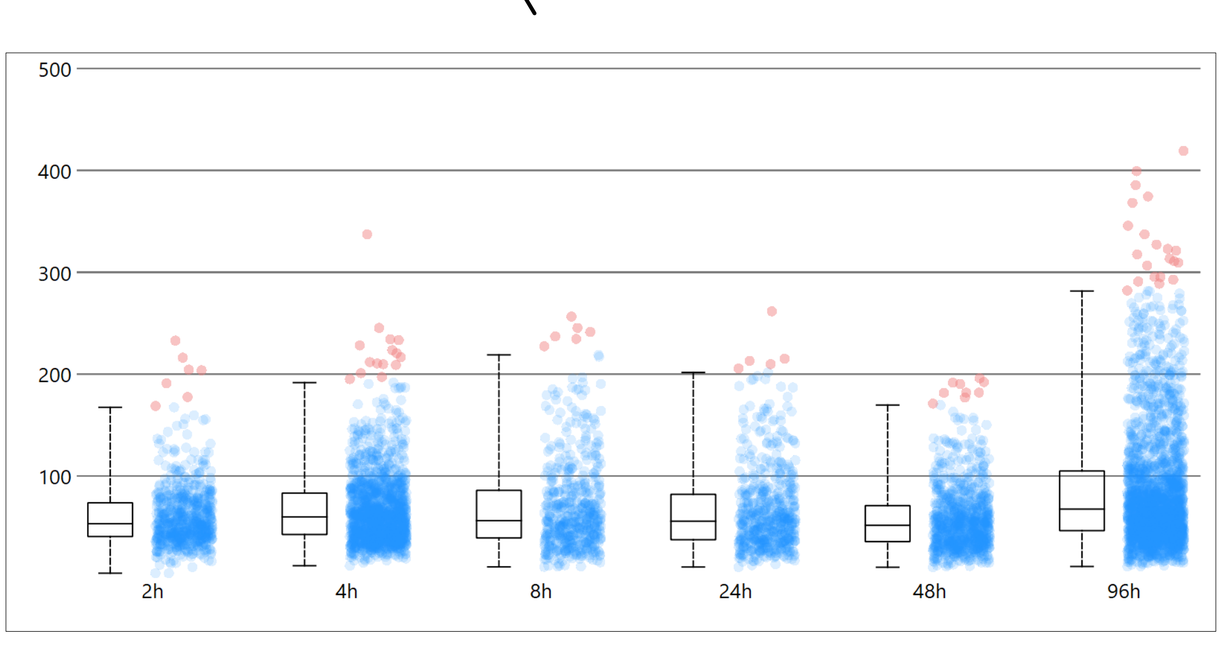

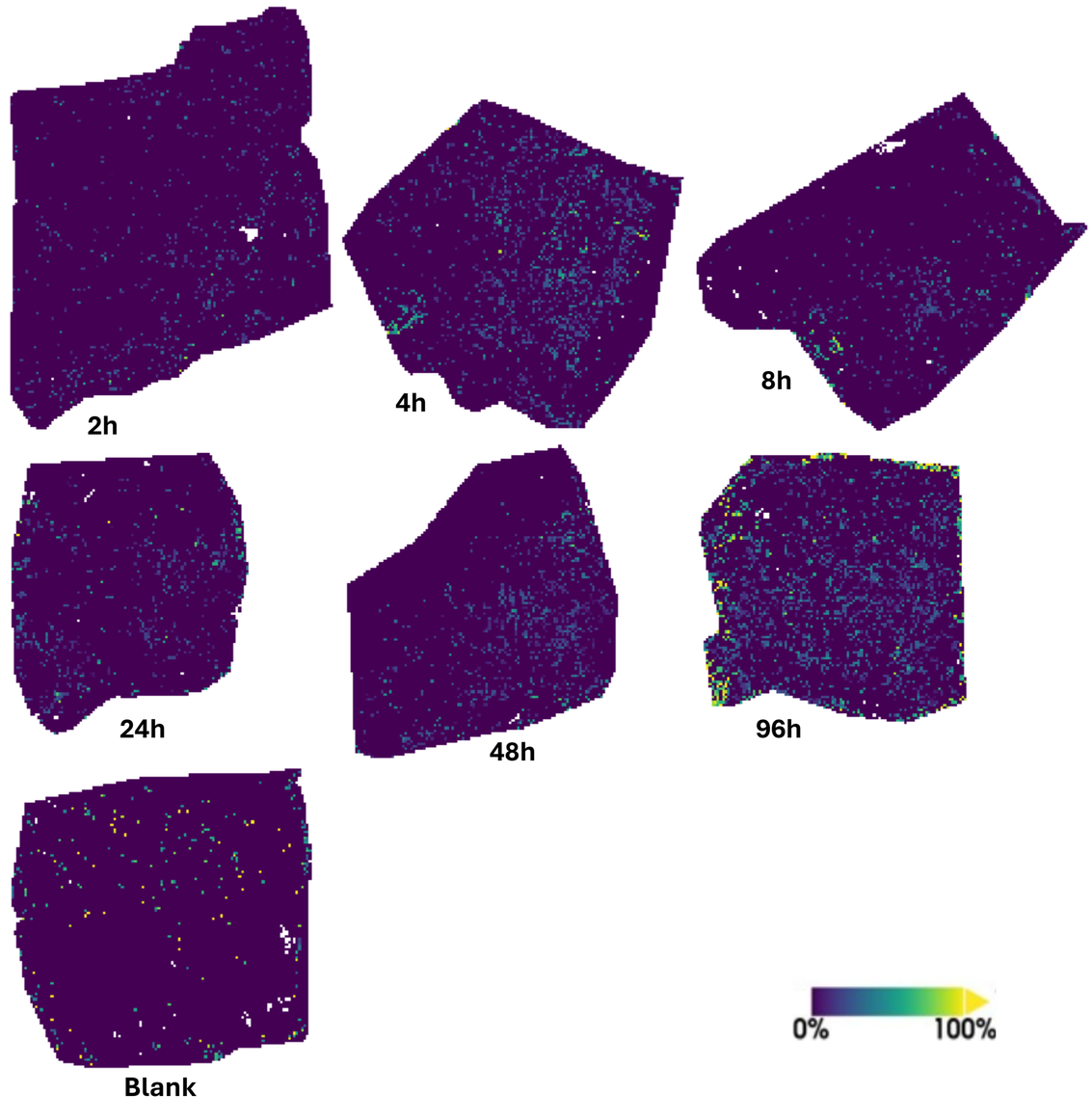

Supplementary Fig. 3n) MS Ion images of BAC4-OH over the time-course of 2, 4, 8, 24, 48, 96 h

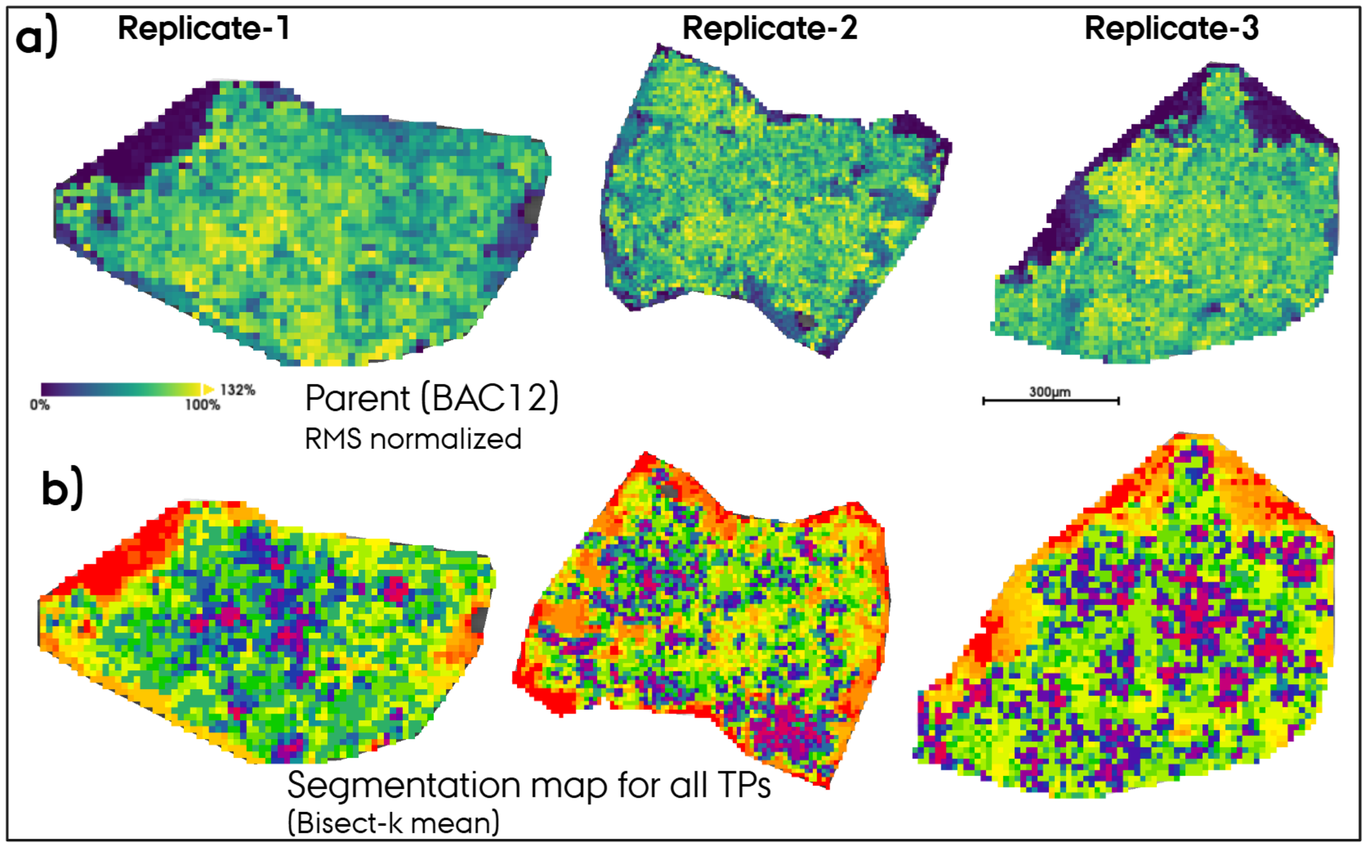

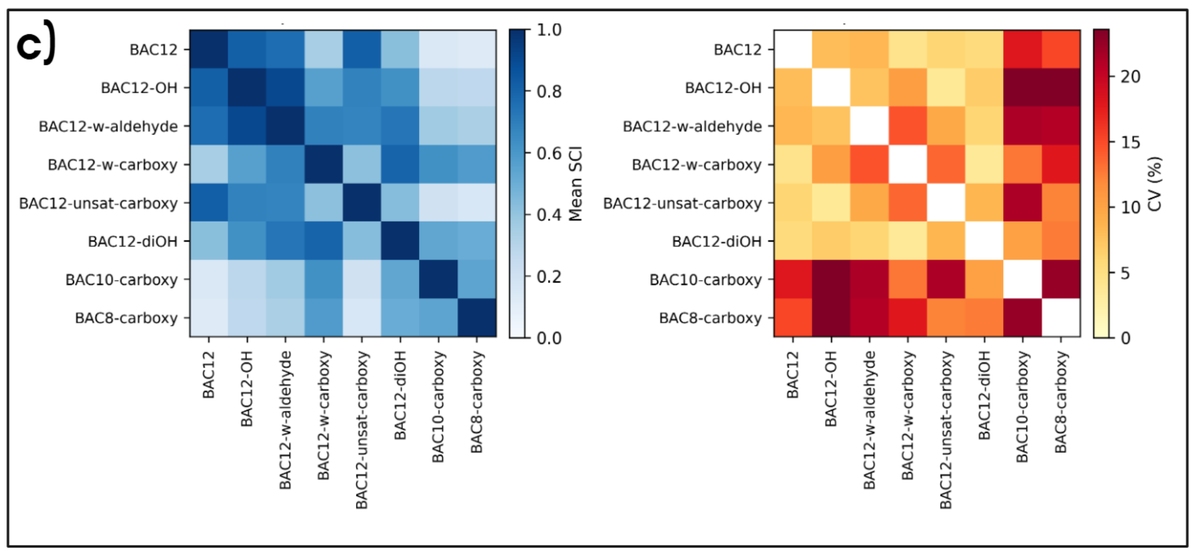

Mean SCI (n=3) correlation matrix and respective CVs

Supplementary Fig. 4) a)Reproducibility of BAC-12 transformation products (TPs) spatial co-localization across independent biofilm replicates (4 h, n = 3). a) RMS-normalized parent BAC-12 ion images, b)bisecting k-means segmentation maps for all TPs, c) mean spatial co-localization index (SCI) and corresponding coefficient of variation (CV, %) across replicates for the seven TPs. MS Spectral clusters are color coded across replicates.

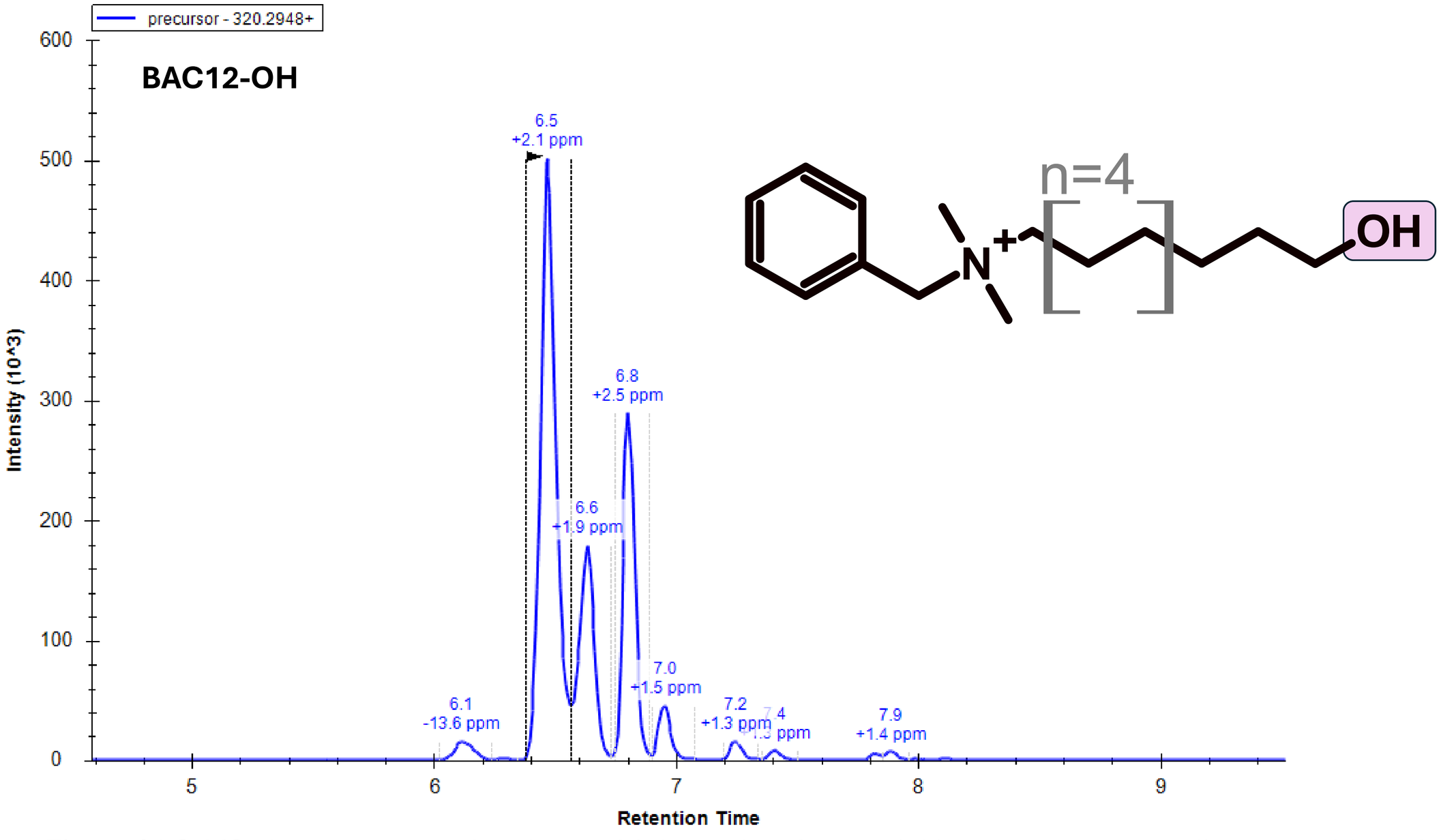

Supplementary Fig. 5a) LC-MS chromatogram showing multiple peaks of potential isomers corresponding to position of –OH group positions.

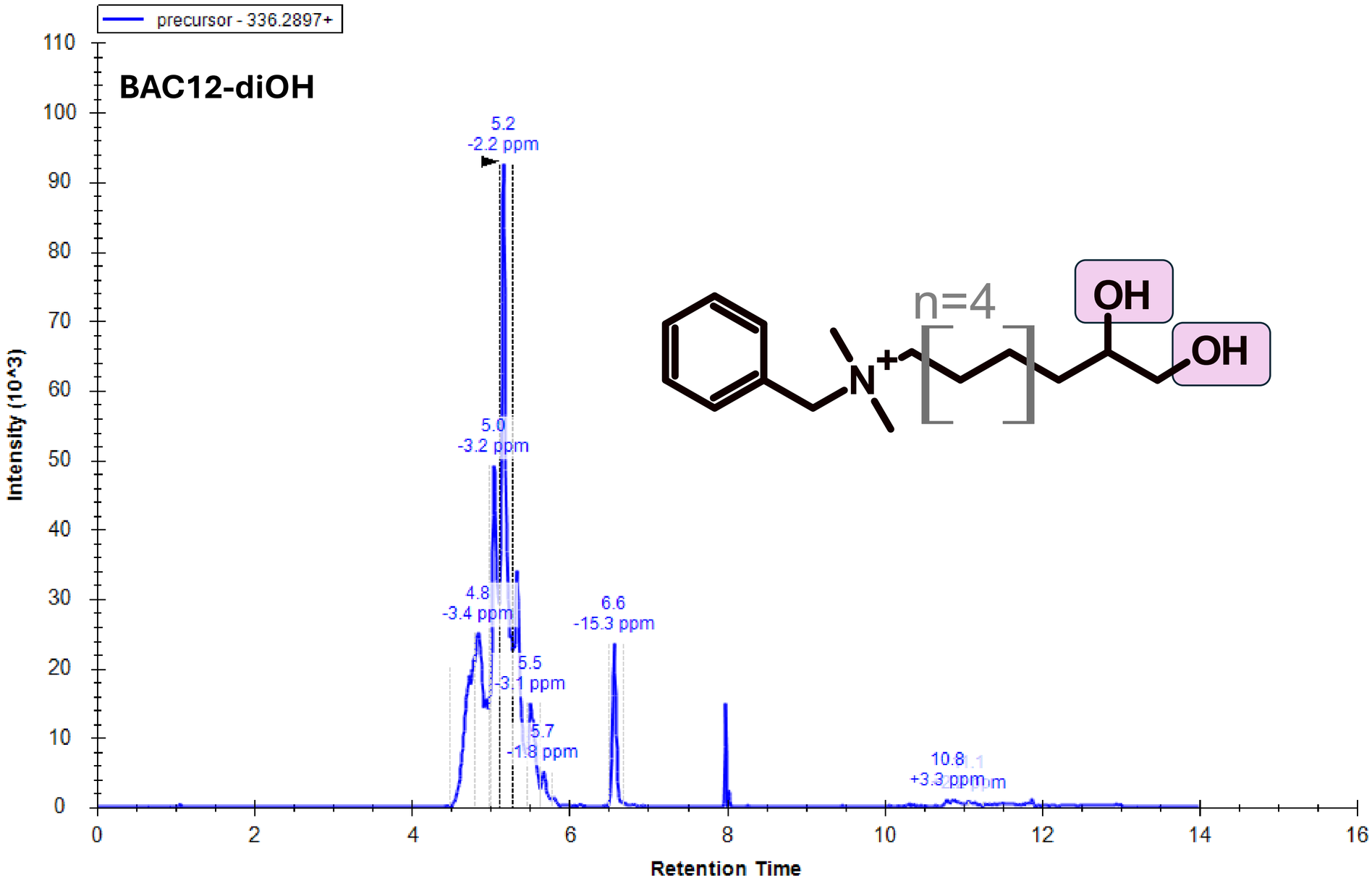

Supplementary Fig. 5b) LC-MS analysis showing multiple peaks for potential isomers corresponding to position of di-OH group positions.

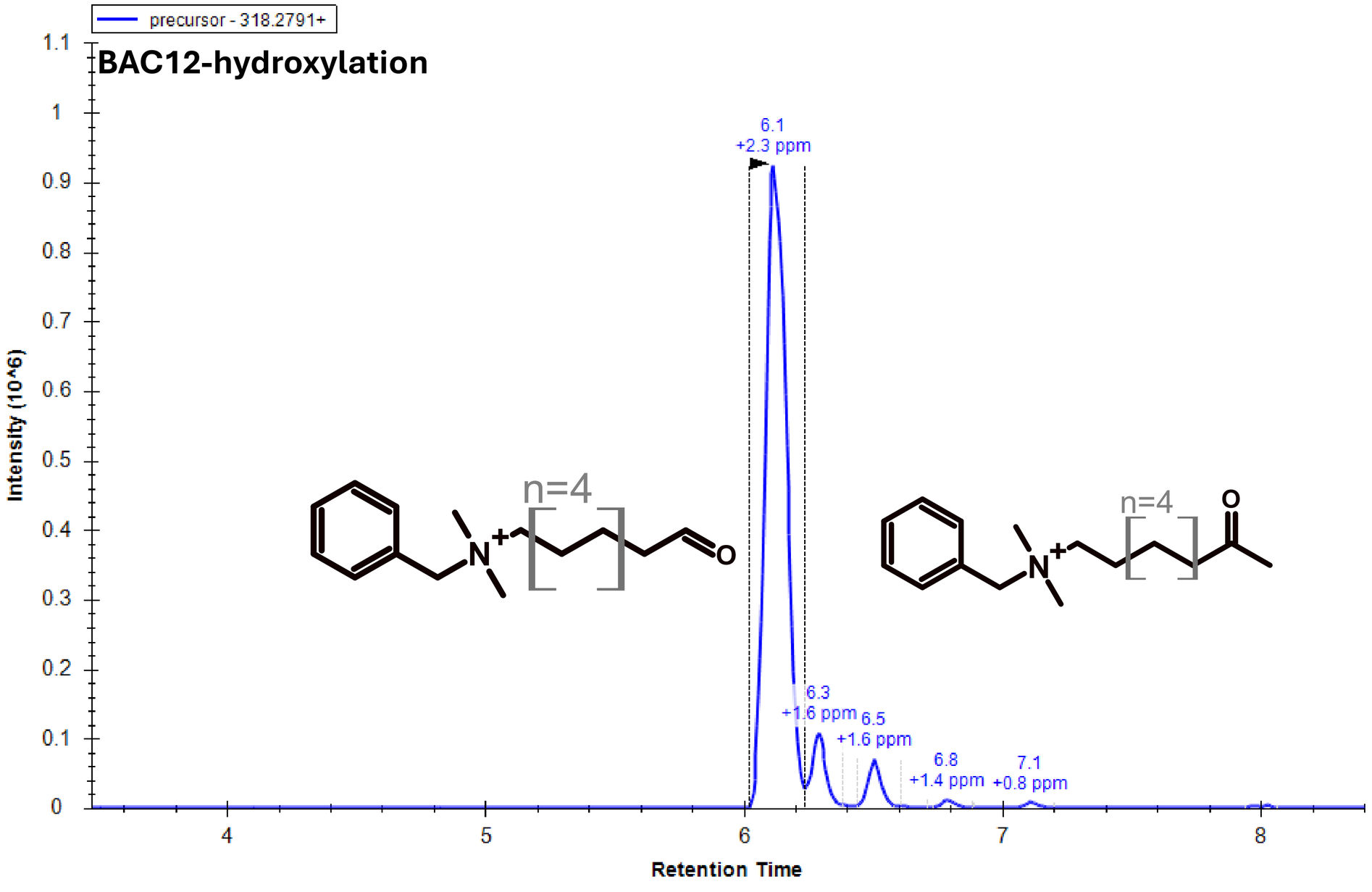

Supplementary Fig. 5c) LC-MS chromatogram showing multiple peaks for potential isomers corresponding to position of =O group

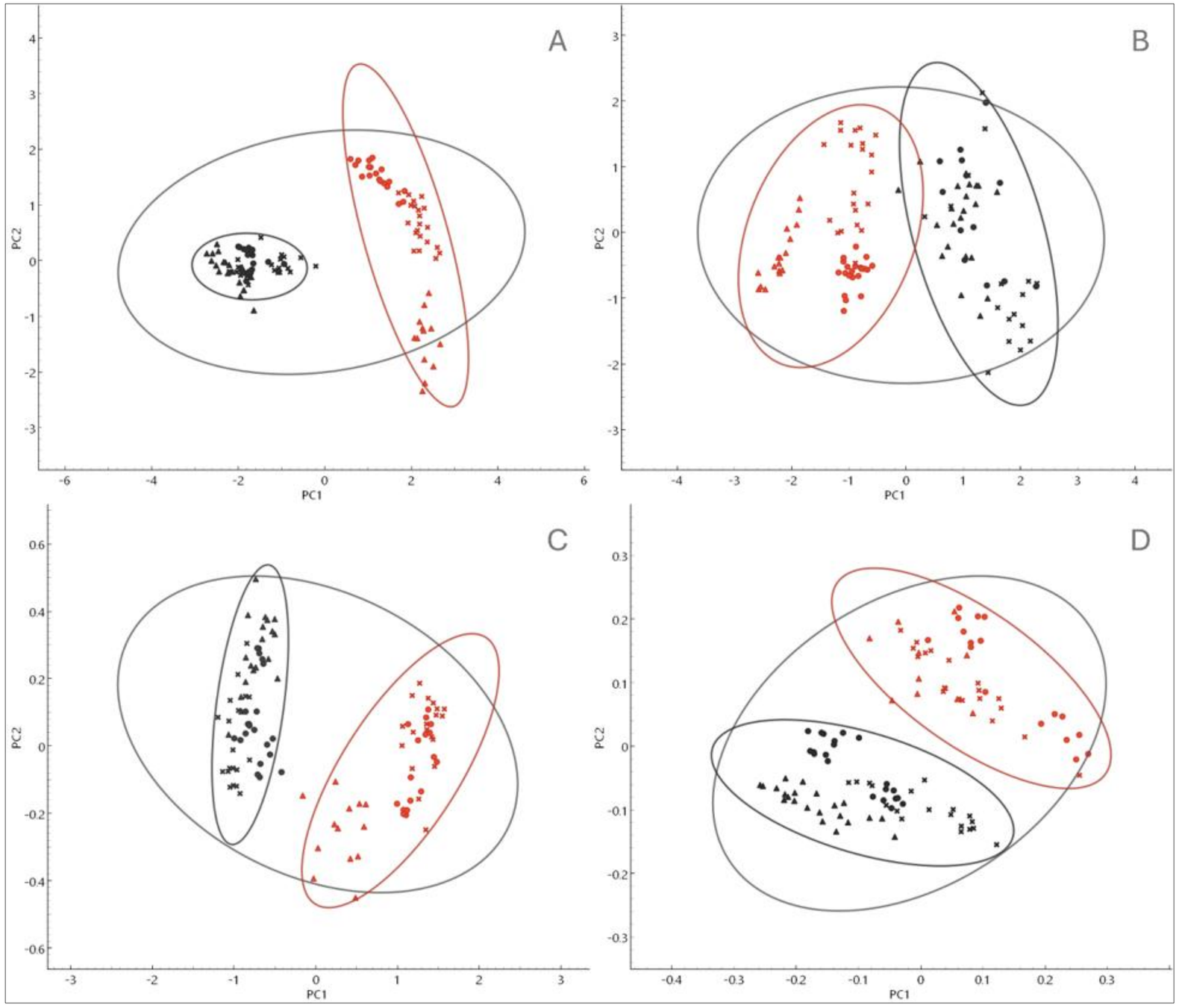

Supplementary Fig. 6) PCA analysis of 20 representative spectra from each of the high-protein regions (A), high-polysaccharide regions (B), the Amide I + Amide II region (C), and the Amide I region alone (D), for both blank (black) and 4 h-treated (red) samples across replicates. Spectra from replicates 1, 2, and 3 are denoted by different symbols (✕, ●, and ▲, respectively).

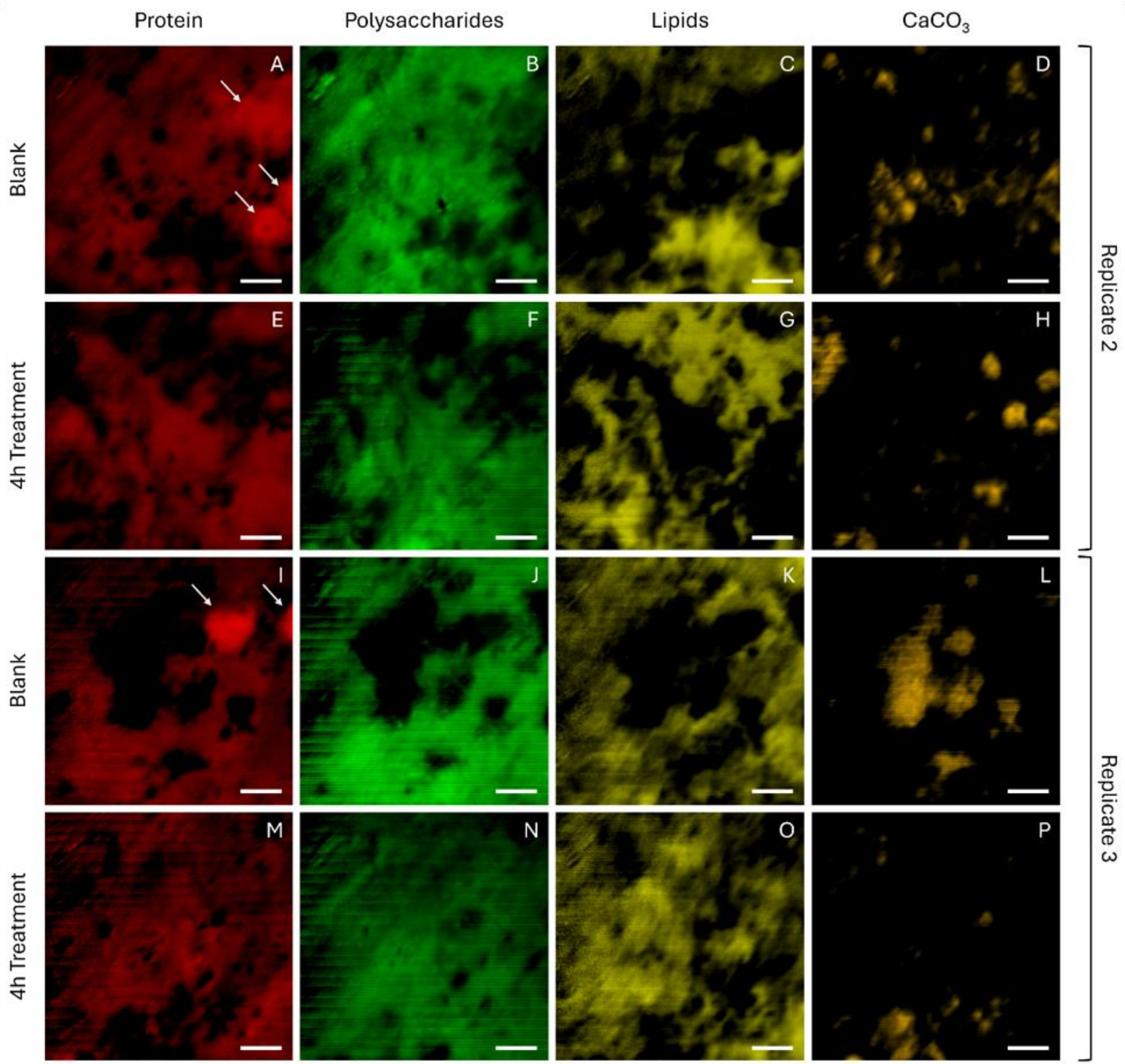

Supplementary Fig. 7) FTIR imaging intensity maps showing the spatial distribution of protein (red), polysaccharides (green), lipids (yellow), and $CaCO_3$ (orange) in the blank sample (A–D and I-L) and after 4 h of treatment (E–H and M-P) for both replicate 2 and 3. Each map was generated from the integrated intensity of a characteristic band: protein at 1640 cm^{-1}, polysaccharides at 1055 cm^{-1}, lipids at 1722 cm^{-1}, and $CaCO_3$ at 872 cm^{-1}. White arrows indicate protein aggregates detected in the blank samples. Each image covers a 300 × 300 µm area (scale bar: 50 µm).